LASER BEAM SCINTILLATION IN THE MARINE BOUNDARY LATER

Brian Christian Haagensen

NAVAL POSTGRADUATE SCHOOL
Monterey, California

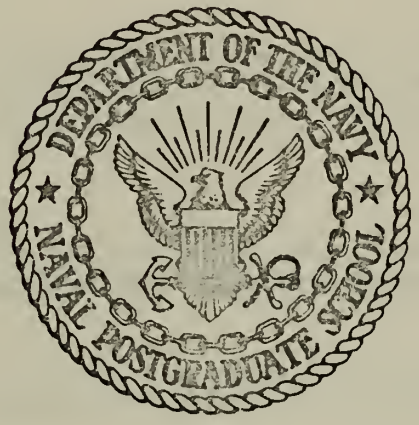

THESIS

LASER BEAM SCINTILLATION
IN THE
MARINE BOUNDARY LAYER

by

Brian Christian Haagensen

Thesis Advisor: A. W. Cooper

June 1973

Approved for public release; distribution unlimited.

Laser Beam Scintillation in the Marine Boundary Layer

by

Brian Christian Haagensen
Ensign, United States Navy
B.S., United States Naval Academy, 1972

Submitted in partial fulfillment of the
requirements for the degree of

MASTER OF SCIENCE IN PHYSICS

from the

NAVAL POSTGRADUATE SCHOOL
June 1973

ABSTRACT

Intensity scintillation in a laser beam at 0.63 micrometers in the marine boundary layer has been studied over a 4.3 kilometer horizontal path across Monterey Bay and also from shore to ship at San Nicolas Island. Optical and micrometeorological measurements of the refractive index structure constant, C_N, agree to approximately one standard deviation giving values in the range 2.0×10^{-8} to $5.0 \times 10^{-}$ $(\text{meters})^{-1/3}$. Optical and meteorological data correlation improved as mean wind speed increased. Evidence was found to support the reported existence of a saturation region for the laser beam logarithmic amplitude variance.

TABLE OF CONTENTS

LIST OF GRAPHS

LIST OF FIGURES

LIST OF DATA TABLES

ACKNOWLEDGEMENTS

The scope of this project required the participation of a large number of personnel. The author would like to thank those people without whose support, this research would not have been possible.

The project benefited from the support of the Office of Naval Research through the Naval Postgraduate School's Foundation Research Program and the Naval Ordnance Laboratory. The cooperation of the managements of the Monterey Holiday Inn and the Hopkins Marine Station (of Stanford University) was greatly appreciated. They provided rooms and electrical power for the laser and scintillometer systems.

The Directorate of Industrial Operations at Fort Ord provided the radios used for establishing communications between measurement stations. Without these radios, coordination of the measurements would have been nearly impossible.

During the San Nicolas Island experiment, the assistance rendered by Mr. G. Gibbs, Mr. J. Karney and Mr. M. Oberg of the Naval Missile Center, Point Mugu, was invaluable. They arranged for range clearances, made independent optical measurements of atmospheric turbulence and assisted the optical research team in making ship-to-shore scintillation measurements.

The Oceanographer of the Navy provided the facilities of the oceanographic research vessel Acania. The cooperation

of the Naval Postgraduate School's Oceanography Department and the captain and crew of the Acania was greatly appreciated.

The meteorological research group was headed by Dr. Kenneth Davidson of the Meteorology Department. Included in this group were Dr. Thomas Houlihan of the Mechanical Engineering Department and Dr. Noel Boston of the Oceanography Department. This group has been responsible for the meteorological experimentation and analysis constituting the other half of the coordinated propagation study project, of which the work here described has been a part. The significance of the results is equally dependent on the meteorological and optical measurements.

The optical research team was headed by Professor Eugene Crittendon of the Physics Department until his departure for Australia in January. Professor Alfred Cooper headed the optical team in his absence. Included in the optical research team were Professor Fred Buskirk, Professor Sydney Kalmbach and Professor Raymond Kelly, all of the Physics Department. These men spent many hours designing and running the optical experiments. In addition, Lieutenant Arthur Schroeder and Lieutenant David Beall, both graduate students in physics, gave many hours of their time helping to make measurements during the second Monterey Bay experiment. These men will be continuing the optical research effort as their masters thesis project. The author wishes them much success.

Technical help for the project was provided by Mr. Robert Moehler, Mr. Lynn May and Mr. Thomas Christian. Their practical expertise in making systems work properly was greatly appreciated.

A special word of thanks is richly deserved by my thesis advisor, Dr. Alfred Cooper. His participation, help and encouragement in the face of numerous "crises" contributed a large part to the results and successes of this research effort.

Finally, my wife, Valerie, deserves special acknowledgement for her efforts in transporting equipment and especially for her moral support.

I. INTRODUCTION

Atmospheric effects on laser beam propagation are divided into three general categories: refraction, absorption, and particulate scattering. This investigation was exclusively concerned with atmospheric refraction effects. Refraction may be further subdivided into large-scale refraction, where the beam's spatial path is altered, and small-scale refraction, where the beam is differentially focused and defocused. Large-scale refraction, commonly referred to as beam wander, was found to be negligible. All research efforts were directed toward the small-scale refraction phenomenon commonly referred to as beam or atmospheric scintillation.

The major purpose of the research was to make and to correlate direct optical measurements of laser beam scintillation with meteorological measurements of certain atmospheric parameters. Using Rytov's method as described by Tatarski [1], the optical and meteorological measurements of beam scintillation were compared by calculating the atmospheric refractive index structure constant which statistically describes atmospheric refractive index fluctuations. The research team attempted to predict laser beam scintillation by making micrometeorological measurements of atmospheric parameters.

The project effort consisted of two primary areas, an optical determination of the refractive index structure

constant (C_{NO}) and a meteorological determination of the refractive index structure constant (C_{NT}). These measurements were made simultaneously and compared for correlation. This experiment differs from previous experiments conducted by Livingston [2], Ochs [3] and Fitzmaurice [4] in that the laser path was over the ocean instead of over land.

This research project was funded by the Naval Ordnance Laboratory and was divided into two related areas, meteorology and optics. The meteorological research group, headed by Dr. Kennet. Davidson of the Naval Postgraduate School, made and evaluated the micrometeorological measurements of atmospheric turbulence. The optical research group, headed by Dr. Eugene Crittendon (until his departure for Australia in January) and later by Dr. Alfred Cooper, made and evaluated the optical measurements of laser beam scintillation.

Due to the wide extent of each of the areas of investigation, each group worked independently of the other to obtain an estimate of atmospheric turbulence. These estimates were compared for correlation after data reduction and analysis. The inherent nature of this organization promoted specialization of the personnel involved in either the optical or meteorological areas of research. The author, by virtue of his background in electro-optics, concentrated his efforts in optical research. Hence, this report is devoted primarily to the procedures and conclusions of the optical research group. This thesis represents a comprehensive

description of the efforts and results of the optical propagation study. Meteorological techniques and experimental results are described briefly when they relate to optical data.

II. PROJECT BACKGROUND

A. HISTORICAL SUMMARY

The earliest observations of scintillation in a light beam propagating through the atmosphere were made by ancient astronomers who noticed the "twinkling" of stellar images. Stellar scintillation was measured quantitatively by Middleton in 1949 [5] and 1952 [6]. Chandrasekhar, in 1952 [7], estimated the phase and amplitude fluctuations of starlight caused by atmospheric turbulence by means of a geometrical optics approach. In 1953, Mintzer [8] applied the Born approximation to the scalar wave equation to describe the propagation of sound waves through a turbulent ocean, a problem similar to the propagation of light through a turbulent atmosphere.

Muchmore and Wheelon [9], in 1955, used Chandrasekhar's approach to study line of sight propagation of radio waves in the troposphere. They calculated the variance and spatial correlation functions for the amplitude and the phase of the propagating wave. Two articles by Wheelon published in 1959 [10, 11] review the state of the art of wave propagation at that time. These articles cover turbulence theory and atmospheric propagation of radio waves which is a similar problem to propagation of optical beams.

In 1960 and 1961, the Russian monographs by Chernov [12] and Tatarski [1] were translated into English. These works

described the method proposed by Rytov [14] (see Section III.D for the derivation) for analyzing the diffraction of light by ultrasonic waves and later applied by Obukov [15] to the propagation of light waves through a turbulent atmosphere. Strohbehn [16] presents a good discussion on the range of validity and approximations made by Rytov's method. The calculations in this project were based on Tatarski's formulation of Rytov's method. Rytov's method takes into consideration multiple scattering and diffraction effects and thereby represents a significant advancement in the theory of atmospheric propagation of planar or spherical electromagnetic waves. Strohbehn's article, published in 1968, is an excellent review of atmospheric propagation theory.

Lumley and Panofsky [17] wrote (in 1964) a monograph covering many facets of turbulence theory as applied specifically to the atmosphere. This defined the meteorological theory used by the Naval Postgraduate School's research group to obtain estimates of the atmospheric refractive index structure constant. In 1972, Davidson, in a Naval Postgraduate School report [18], comprehensively described the meteorological measurements made and the theory applied in this project. Articles by Wyngaard (et al.) in 1971 and Panofsky [19, 20] in 1968 provide further references on meteorological turbulence theory as applied by the research group.

B. RECENT DEVELOPMENTS

In his monograph, Wave Propagation in a Turbulent Medium [1], Tatarski reported the results of some of the earliest experiments that compared micrometeorological estimates to optical estimates of atmospheric turbulence using Rytov's method. These experiments were performed in the late 1950s using an incoherent light source. The propagation path ranged from 250 to 2000 meters over a Russian steppe. Experimental results strongly supported his formulation of propagation theory. The fluctuations of beam intensity and phase caused by atmospheric turbulence were found to have a log-normal probability distribution. Tatarski's description of the scintillation frequency spectrum and the dependence of the fluctuation variance on path length were found to match propagation measurements.

In 1966, Schmeltzer [22] published a derivation of the covariance of the logarithmic intensity and phase fluctuations of a propagating beam of light. His results were more general than Tatarski's as they are valid for collimated and focused beams as well as plane and spherical waves. However, his results were in the form of complicated double integral equations and so were not directly useable. Fried evaluated these integrals to obtain analytic expressions for the logarithmic intensity variance of a spherical wave [23] and for a collimated or focused beam [24]. His expression for spherical wave scintillation was in agreement with Tatarski's results.

In 1969, Ochs [3] repeated Tatarski's experiments in Colorado using a helium-neon laser as a light source. His experiment found several deviations from Tatarski's theory including the existence of a saturation region for the optical measurements. When atmospheric turbulence was very high, Ochs found that meteorological measurements would continue to measure turbulence values but the optical measurements would saturate at a lower turbulence value. Optical and meteorological measurements would not correlate until the turbulence had decreased below the saturation level of the optical measurements.

Similar experiments were performed over land by Fitzmaurice in 1970 [4] and by Dowling and Livingston in 1971 [2]. Both groups measured the scintillation of 0.6328 and 10.6 micrometer laser beams and compared optical and micrometeorological estimates of atmospheric turbulence. Both groups found evidence of a saturation region.

The work described in this thesis was part of an interdepartmental program formed as a combination of the efforts of existing optical and meteorological research groups at the Naval Postgraduate School. This study applied Tatarski's formulation of Rytov's method to describe atmospheric turbulence. Optical and micrometeorological measurements of laser beam scintillation and atmospheric temperature fluctuations have been made independently and then analyzed. Both types of measurement yielded values for the index of refraction

structure constant, C_N. Theory predicts that if the turbulence is isotropic and homogeneous, these values of C_N should be equal. However, two major unresolved questions remained. First, does saturation of optical values of C_N exist in the high turbulence regime? If so, what parameters determine this saturation? Ochs [3] reported that the saturation level seemed to vary with mean wind speed and the time of day.

Second, Friehe, of Scripps Institute, reported recently that humidity fluctuations, which were neglected by Tatarski, may contribute significantly to refractive index fluctuations in the atmosphere [25]. His findings have not been generally accepted by propagation researchers. The frequency response of available humidiometers is inadequate to check these predictions.

Although considerable evidence exists to support Tatarski's propagation theory over land, the problem of propagation in the marine environment has not been resolved. If humidity variations influence refractive index fluctuations, laser propagation over the ocean may not be described by Tatarski's formulation of Rytov's method. This thesis examines the validity of Tatarski's propagation theory in the marine boundary layer.

III. THEORY

A. GENERAL REMARKS

Atmospheric turbulence is a three-dimensional, nonlinear, stochastic process that occurs in air whenever certain fluid-mechanical parameters are exceeded. Random, dissipative fluctuations in the homogeneity of the atmosphere will cause the velocity profiles of the air to vary in time and space. These fluctuations have significant effects on the propagation of a laser beam by continuously changing atmospheric density. This causes the refractive index to fluctuate with time and space.

Atmospheric turbulence (linear) effects on laser beam propagation may be classified into two categories. Large-scale inhomogeneities will uniformly refract the laser beam and cause the beam to wander in space. Small-scale inhomogeneities will differentially refract the laser beam and cause interference phenomena or scintillation. Small-scale turbulence alters the optical path length over different segments of the beam and generates interference patterns between adjacent wave fronts. This alters the initial phase and amplitude distributions of the propagating beam and destroys spatial and temporal coherence.

Due to the inherent causes of turbulence, it is impossible to predict the transient velocity fields that arise for a given set of boundary flow conditions. Statistical analysis

must be used to describe atmospheric turbulence. By analyzing the variations in atmospheric homogeneity, one may describe the fluctuations of the index of refraction over a given path.

Relating the fluctuations in a propagating laser beam to atmospheric turbulence is a three-part problem. The first part is to find a convenient formulation for characterizing atmospheric turbulence. This may be done by using statistical estimators of the covariance and the structure function to describe fluctuations in the index of refraction. The second part of the problem is to derive the equations that govern the propagation of electromagnetic waves through a random medium, starting with Maxwell's equations. These equations will relate the magnitude and phase of the radiation to the index of refraction of the optical path. The final part of the problem is to combine the statistical description of the index of refraction with the propagation equation. The result will be an analytic relationship between the statistical description of the refractive index and a statistical description of the phase and amplitude of the propagating beam.

The entire derivation is extremely long and difficult. Consequently only the physically most important points of the derivation are discussed here, and much of the turbulence theory and mathematics are omitted. A complete treatment of the propagation problem may be found in references 1, 17, 22, 23 and 24.

In order to minimize the effects of beam wander on the scintillation measurements, the laser beam was diverged. The propagating diverged beam was approximated by a spherical wave. Thus the general propagation equations obtained were evaluated for the case of a spherical wave.

B. TURBULENCE THEORY

Wave propagation in a random continuous medium is governed by a stochastic wave equation, whose index of refraction, $n(\bar{r},t)$, is a continuous random point function, and characterizes the transmission medium. For line of sight propagation on the earth, optical paths are relatively short enabling one to say that the transit time of a given phase front between the source and receiver is much less than the time constant associated with changing spatial distribution of the refractive index (typically 10^{-3} seconds). The time dependence of $n(\bar{r},t)$ will be accounted for by letting each $n(\bar{r},t_i)$, for $i = 1, 2, 3...$ be considered a single realization of the random process, $n(\bar{r})$. Hence, one can characterize the transmission medium by a refractive index in the form

$$(1) \qquad n(\bar{r}) = \langle n(\bar{r}) \rangle + n_1(\bar{r}) \cong 1 + n_1(\bar{r})$$

where $n_1(\bar{r})$ represents the fluctuations in $n(\bar{r})$.

Tatarski [1] assumed that the power spectrum of the turbulence, $\Phi_n(K)$, can be described by the empirical Kolomogorov model where

(2) $$\Phi_n(K) = 0.033\, C_N^2\, K^{-11/3} \exp(-K^2/K_m^2) .$$

C_N is a constant that parameterizes the total amount of energy in the turbulence. Tatarski showed that C_N can be related to a statistical estimator by

(3) $$D_n(d) = C_N^2\, d^{2/3}$$

where $D_n(d)$ is the structure function of the refractive index given by

$$D_n(d) = \langle [n(r) - n(r+d)]^2 \rangle$$

and hence

(4) $$C_N^2 = \frac{\langle [n(r) - n(r+d)]^2 \rangle}{d^{2/3}} .$$

Assuming isotropic, homogeneous turbulence, the functional arguments $\bar{r}$ and $\bar{d}$ can be changed from vectors to scalar distances.

The quantity K, the spatial wave number, is given by $K = 2\pi/\ell$ where ℓ is commonly interpreted, in some sense, as the size of the turbulent eddy. This turbulence spectrum is valid for values of K that are in the inertial subrange, that is, the range where $\ell_0 < \ell < L_0$. The inner scale, ℓ_0, characterizes the size of turbulent eddies where viscous dissipation of turbulent energy becomes predominant (for values of ℓ less than ℓ_0). K_m is the spatial wave number corresponding to the inner scale (i.e., $K_m = 2\pi/\ell_0$). Values

of ℓ greater than the outer scale, L_0, characterize the region of the turbulence spectrum where the eddies are not homogeneous and where energy is added to the turbulence spectrum. For values of ℓ in the inertial subrange, the motion of the larger turbulent eddies causes the formation and transfer of energy to smaller eddies with very little viscous dissipation. These eddies then form and transfer energy to smaller eddies and so on until eventually, at approximately $\ell = \ell_0$, viscous effects become the predominant method of energy dissipation and turbulent energy is converted to thermal energy. Typically, for atmospheric turbulence in the marine boundary layer, ℓ_0 is of the order of a few millimeters and L_0 is of the order of a few meters (depending on the stability conditions and height above the boundary).

Turbulence theory shows that the covariance of the refractive index for homogeneous, stationary conditions

$$C_n(d) = \langle n(r+d)\, n(r) \rangle \tag{5}$$

is the three-dimensional Fourier transform of the turbulence energy spectrum

$$C_n(d) = 4\pi/d \int_0^\infty \Phi_n(K)\, K \sin(Kd)\, dK \,. \tag{6}$$

Also, the structure function of the index of refraction, given by equations (3) and (4), is related to the turbulence

energy spectrum by the transform relation

$$(7) \qquad D_n(d) = 8\pi \int_0^\infty \left(1 - \frac{\sin(Kd)}{Kd}\right) \Phi_n(K)\, K^2\, dK$$

under conditions of isotropy, homogeneity and stationarity. Given equations (2) and (6), one can relate $C_n(r)$ to C_N. This means that C_N can be used to describe the statistics of the fluctuations of the refractive index in the atmosphere.

C. DERIVATION OF THE SCALAR WAVE EQUATION

The equations describing the propagation of an electromagnetic wave in the atmosphere are derived from Maxwell's equations for a non-conducting medium without charge sources.

$$(8) \qquad (a) \quad \bar{\nabla} \cdot \bar{D} = 0$$

$$(b) \quad \bar{\nabla} \cdot \bar{B} = 0$$

$$(c) \quad \bar{\nabla} \times \bar{E} = -\frac{\partial \bar{B}}{\partial t}$$

$$(d) \quad \bar{\nabla} \times \bar{H} = \frac{\partial \bar{D}}{\partial t}$$

with the additional relations

$$(e) \quad \bar{D} = \varepsilon \bar{E} \qquad \text{with } \varepsilon = \varepsilon(\bar{r})$$

$$(f) \quad \bar{B} = \mu \bar{H} \qquad \text{with } \mu = \mu_o = \text{constant.}$$

Taking the curl of equation (8c) one gets

$$(9) \qquad \bar{\nabla} \times \bar{\nabla} \times \bar{E} = \bar{\nabla}(\bar{\nabla} \cdot \bar{E}) - \nabla^2 \bar{E} = \mu \bar{\nabla} \times \frac{\partial \bar{H}}{\partial t} \ .$$

Assuming a time dependence of $e^{-i\omega t}$ for all field quantities and substituting equation (8d) into the right hand side of

equation (9), one finds

$$(10) \quad \bar{\nabla}(\bar{\nabla} \cdot \bar{E}) - \nabla^2 \bar{E} = -\mu \frac{\partial(\bar{\nabla} \times \bar{H})}{\partial t} = -\mu \frac{\partial}{\partial t} \left(\frac{\partial \bar{D}}{\partial t}\right)$$

$$= -\mu\varepsilon \frac{\partial^2 \bar{E}}{\partial t^2}$$

$$= \mu\varepsilon\omega^2 \bar{E} \ .$$

Starting with Maxwell's equation (8a) and using a well known identify for the divergence operator,

$$(11) \quad \bar{\nabla} \cdot \bar{D} = \bar{\nabla} \cdot \varepsilon\bar{E} = \varepsilon\bar{\nabla} \cdot \bar{E} + \bar{E} \cdot \bar{\nabla}\varepsilon = 0$$

or

$$(12) \quad \bar{\nabla} \cdot \bar{E} = -\frac{\bar{E} \cdot \bar{\nabla}\varepsilon}{\varepsilon} \ .$$

Substituting equation (12) into equation (10) gives

$$(13) \quad \nabla^2 \bar{E} + \mu\varepsilon\omega^2 \bar{E} = -\bar{\nabla}\left(\frac{\bar{E} \cdot \bar{\nabla}\varepsilon}{\varepsilon}\right) \ .$$

The index of refraction for a medium is given by

$$(14) \quad n = \frac{c}{V} = c(\mu\varepsilon)^{1/2} = (\text{const})(\varepsilon)^{1/2}$$

where c equals the velocity of propagation in free space, V equals the velocity of propagation in the medium and the wave number is given by

$$(15) \quad k = \frac{\omega}{c} \ .$$

Hence

$$\omega^2\mu\varepsilon = \left(\frac{\omega^2}{c^2}\right)(c^2\mu\varepsilon) = k^2 n^2 \qquad \text{and} \tag{16}$$

$$\nabla^2 \bar{E} + k^2 n^2 \bar{E} = -\bar{\nabla}\left(\frac{\bar{E} \cdot \bar{\nabla}\varepsilon}{\varepsilon}\right) . \tag{17}$$

Realizing from equation (14) that $n^2 = (\text{const})\varepsilon$, then $\frac{\bar{\nabla}\varepsilon}{\varepsilon} = \frac{\bar{\nabla}n^2}{n^2} = 2\bar{\nabla}\ln(n)$ and equation (17) becomes

$$\nabla^2 \bar{E} + k^2 n^2 \bar{E} = -2\bar{\nabla}[\bar{E} \cdot \bar{\nabla}\ln(n)] . \tag{18}$$

The term $-2\bar{\nabla}[\bar{E} \cdot \bar{\nabla}\ln(n)]$ couples the various components of the field together and is responsible for polarization fluctuations in the linearly polarized beam. Fitzmaurice [4] shows that if the deviations of the refractive index from its mean value is very small (typically $n_1/\langle n\rangle \sim 10^{-6}$) and if the wavelength of the propagating wave is much less than the inner scale (ℓ_0) of the turbulence, then one can assume that the polarization fluctuation term is negligible. This gives the scalar wave equation

$$\nabla^2 E + k^2 n^2 E = 0 \tag{19}$$

where E is any rectangular component of $\bar{E}(\bar{r})$.

D. RYTOV'S METHOD

At this point, Rytov [14] transformed equation (19) to

$$\nabla^2 \ln(E) + |\bar{\nabla} \ln(E)|^2 + k^2 n^2 = 0 . \tag{20}$$

Now let

$$E(\bar{r}) = A(\bar{r}) \exp[iS(\bar{r})] \tag{21}$$

and from equation (1), $n(\bar{r}) = 1 + n_1(\bar{r})$.

Define the complex phase, ψ, as

$$E(\bar{r}) = \exp[\psi(\bar{r})] = \exp[\ln A(\bar{r}) + iS(\bar{r})] \tag{22}$$

and therefore,

$$\ln(E) = \ln(A) + iS = \psi(\bar{r}). \tag{23}$$

Substituting this result into equation (20) gives

$$\nabla^2 \psi + |\nabla \psi|^2 + k^2 (1 + n_1)^2 = 0. \tag{24}$$

Now set

$$\psi = \psi_o + \psi_1 \quad \text{so that} \tag{25}$$

$$E = \exp(\psi_o + \psi_1) = E_o \exp(\psi_1) . \tag{26}$$

E_o is the unscattered wave which satisfies the equation

$$\nabla^2 E_o + k^2 E_o = 0 \tag{27}$$

or the transformed equation

$$\nabla^2 \ln(E_o) + |\bar{\nabla} \ln(E_o)|^2 + k^2 = 0. \tag{28}$$

Substituting equation (22) into equation (28),

$$\nabla^2 \psi_o + |\bar{\nabla} \psi_o|^2 + k^2 = 0 . \tag{29}$$

Now, substituting equation (25) into equation (24) gives

$$\nabla^2 \psi_o + \nabla^2 \psi_1 + |\bar{\nabla} \psi_o + \bar{\nabla} \psi_1|^2 + k^2 (1 + 2n_1 + n_1^2) = 0 \tag{30}$$

and subtracting this from equation (29) gives after some manipulation

$$\nabla^2 \psi_1 + |\bar{\nabla} \psi_1|^2 + 2\bar{\nabla} \psi_o \cdot \bar{\nabla} \psi_1 + k^2 (2n_1 + n_1^2) = 0. \tag{31}$$

This is the nonlinear Ricatti equation. Since n_1 is much less than one, $k^2 n_1^2$ is much less than $2k^2 n_1$ and may be neglected. Similarly, since $|\bar{\nabla} \psi_1| << |\bar{\nabla} \psi_o| \sim k$, then $|\bar{\nabla} \psi_1|^2$ is much less than $2\bar{\nabla} \psi_o \cdot \bar{\nabla} \psi_1$ and one can also neglect the $|\bar{\nabla} \psi_1|^2$ term. Finally, one can write equation (31) as

$$\nabla^2 \psi_1 + 2\bar{\nabla} \psi_o \cdot \bar{\nabla} \psi_1 + 2k^2 n_1 = 0 . \tag{32}$$

The assumption that $|\bar{\nabla} \psi_1| << |\bar{\nabla} \psi_o| \sim k$ is the only significant assumption made in Rytov's method. It is equivalent to saying that the change in the variation

of the complex phase, ψ_1, over a distance of about one wavelength in much less than 2π radians. Realizing that the wavelength is much less than the inner scale, ℓ_0, it is difficult to imagine the phase changing significantly in a propagation distance less than ℓ_0. This approximation is generally referred to as the Rytov approximation in the literature.

A new quantity is now defined

$$W = \psi_1 e^{\psi_o} = \psi_1 E_o \tag{33}$$

so that

$$\psi_1 = \frac{W}{E_o} = W\, e^{-\psi_o} \,. \tag{34}$$

Substituting equation (34) into equation (32) and expanding terms gives

$$\nabla^2 W + k^2 W = -2k^2 n_1 E_o \,. \tag{35}$$

This differential equation has the solution

$$W(\bar{r}) = \int_{V'} 2k^2 n_1(\bar{r}')\, E_o(\bar{r}')\, G(\bar{r} - \bar{r}')\, dV' \tag{36}$$

where $G(\bar{r} - \bar{r}')$ is the Green's function

$$G(\bar{r} - \bar{r}') = \frac{\exp[ik(\bar{r} - \bar{r}')]}{4\pi(\bar{r} - \bar{r}')} \quad \text{for a point source.} \tag{37}$$

Therefore,

$$(38)\quad \psi_1(\bar{r}) = \frac{W}{E_o} = \frac{1}{E_o(\bar{r})} \int_{V'} 2\,k^2\, n_1(\bar{r}')\, E_o(\bar{r}')\, G(\bar{r} - \bar{r}')\, dV'.$$

Equation (38) with $n_1(\bar{r})$ as a random continuous function characterizes the scintillation in the propagating wave if $n_1(\bar{r})$ is known analytically.

It is not practical to measure the index of refraction at every point over the optical propagation path. Instead it is necessary to statistically characterize $n_1(\bar{r})$ using the covariance function, $C_n(\bar{r})$. This brings one to the third part of the problem. The statistics of $\psi_1(\bar{r})$ must be calculated starting from equation (38) and the statistical description of the covariance of the refractive index as given by equation (6).

E. APPLICATION OF TURBULENCE THEORY TO THE PROPAGATION EQUATION

After making many transformations, substitutions and integrations, Schmeltzer [22] obtained the statistical expression for the logarithmic amplitude covariance, $C^2_{\ell A}(d)$ for a beam propagating in a random medium which Fried [23] reduced to

$$(39)\quad C^2_{\ell A}(d) = \frac{k^2}{8\pi}\, \mathrm{Re}\, \{ \int_o^z ds \int_o^\infty \Phi_n(K^{1/2})\, J_o(K^{1/2} d\, \frac{s}{z})$$

$$X\, [1 - \exp\, (\frac{Ks(z - s)}{ikz})]\, dK \}$$

for the case of a spherical wave. The quantity "z" is the optical propagation path length and "s" is a dummy variable of integration with the dimensions of length.

Fried integrates this expression for a spherical wave over s and K to obtain the relation

$$C_{\ell A}^2(d=0) = C_{\ell A}^2 = 0.124\, k^{7/6}\, z^{11/6}\, C_N^2 \quad \text{where} \tag{40}$$

$$C_{\ell A}^2 = \left\langle [\ln(A) - \ln\langle A\rangle]^2 \right\rangle \tag{41}$$

and A is the amplitude of the wave function, $|E(\bar{r})|$.

The logarithmic intensity variance, $C_{\ell I}^2$, is a more readily measurable quantity

$$C_{\ell I}^2 = \left\langle [\ln(I) - \ln\langle I\rangle]^2 \right\rangle \tag{42}$$

where I is the intensity of the radiation ($I = A^2$). Thus,

$$\begin{aligned} C_{\ell I}^2 &= \left\langle [2\ln(A) - 2\ln\langle A\rangle]^2 \right\rangle \\ &= 4\left\langle [\ln(A) - \ln\langle A\rangle]^2 \right\rangle \\ &= 4\, C_{\ell A}^2 \quad \text{and} \end{aligned} \tag{43}$$

$$C_{\ell I}^2 = 4[0.124\, k^{7/6}\, z^{11/6}\, C_N^2] \,. \tag{44}$$

or finally

$$C_N = 1.42\, k^{-7/12}\, z^{-11/2}\, C_{\ell I} \,. \tag{45}$$

The foregoing is a brief summary of the major steps in the development of the governing equation for the propagation

statistics of a spherical wave. Much of the detailed mathematics involved in the derivation has been omitted. For the complete derivation, the original papers by Tatarski [1], Schmeltzer [22], and Fried [23] should be consulted. However, the approximations involved in reducing the equations to analytic form are interesting and will be analyzed here.

F. THEORETICAL ASSUMPTIONS

The major assumption that underlies the entire theory is that the turbulence energy spectrum can be described by the empirical Kolomogorov model [equation (4)]. This model was developed in connection with wind tunnel experiments. Meteorological measurements by Tatarski [1], by Wyngaard, Izumi and Collins [19] and by Panofsky [20] verified that it was applicable in the atmospheric boundary layer over the inertial subrange. It was also implicitly assumed that only those turbulent eddies in the inertial subrange contribute significantly to beam scintillation. Eddies with $\ell > L_0$ would tend to cause beam wander. Eddies with $\ell < L_0$ have little effect on the scintillation because viscous forces cause rapid collapse.

The assumption that $\lambda << \ell_0$ was used to justify ignoring the cross polarization term in the scalar wave equation (equation 18). The helium-neon laser used in the experiment had a wavelength of 0.6328 micrometers which is much less than the dimensions of the inner scale (ℓ_0 was of the order of a few millimeters).

In order to use the perturbation technique to express the variations in the index of refraction, the fluctuations in refractive index were assumed to be much smaller than the mean value. Meteorological measurements confirm that the index of refraction in the atmosphere does not increase by more than a few per cent due to density variations; hence, this assumption seems justified.

The assumption that $\lambda^3 z/\ell_0^4 << 1$ is a very weak restriction at optical wavelengths. For a helium-neon laser and an inner scale value of one millimeter, the propagation path would have to be greater than approximately 10^8 meters for this assumption to become invalid.

The final assumption was that turbulence was isotropic and homogeneous. This approximation is valid for large areas with a smooth regular topography. Ocean conditions are conducive to isotropic homogeneous turbulence. This approximation means that a point turbulence measurement can characterize the turbulence over an entire propagation path.

The experimental conditions seemed to satisfy the requirements of Tatarski's, Schmeltzer's and Fried's theory for the propagation of a spherical wave in a random medium. A goal of this experiment was to test the validity of their propation theory in the marine boundary layer.

G. PROBLEM APPLICATIONS

The calculation of C_N from equation (45) required values of the wavelength of the laser beam, the optical path length

and the variance of the logarithmic intensity fluctuations of the laser beam. The wavelength of the laser was known to be 0.6328 micrometers. The optical propagation path length was measured on a nautical chart. Log-intensity variance was measured using the laser scintillometer which is described in the equipment section of this thesis. The calculated values of C_N were designated C_{NO}, indicating that they were derived from optical measurements. These values of C_{NO} were compared with values of C_N that were calculated from meteorological measurements (designated C_{NT}). A brief explanation of the theory and equations that describe the calculation of C_{NT} is appropriate at this point. The meteorological theory is described in detail by Panofsky [20] and by Wyngaard, Izumi and Collins [19].

H. METEOROLOGICAL TURBULENCE MEASUREMENTS

Variations in the index of refraction in the atmosphere are caused by variations in the density of the air. These variations are due to fluctuations in the temperature, pressure, humidity and perhaps gravity waves. Empirical measurements [4] show that the index of refraction at optical wavelengths can be represented by the equation

$$(46) \qquad n(r) = 1.0 + 77.6 \frac{P(r)}{T(r)} \left(1 + \frac{0.0075}{\lambda^2}\right) \times 10^{-6}$$

where atmospheric pressure, P(r) is in millibars, absolute temperature, T(r), is in Kelvins, and wavelength, λ, is in

micrometers. Evaluation of equation (46) at a wavelength of 0.6328 micrometers gives

$$n(r) = 1.0 + 79.0 \frac{P(r)}{T(r)} \times 10^{-6} \quad . \tag{47}$$

It is generally accepted in atmospheric propagation studies that temperature fluctuations are the predominant mechanism causing index of refraction fluctuations in the atmosphere.[1] Equation (4) defines C_N^2 as

$$C_N^2 = \frac{\langle [n(r) - n(r+d)]^2 \rangle}{d^{2/3}} \quad . \tag{4}$$

One can also define a temperature structure constant, C_T^2 by

$$C_T^2 = \frac{\langle [T(r) - T(r+d)]^2 \rangle}{d^{2/3}} \quad . \tag{48}$$

Rearranging terms gives

$$C_N^2 = \frac{\left\langle \left[\left(79.0 \frac{P}{T(r)} \times 10^{-6}\right) - \left(79.0 \frac{P}{T(r+D)} \times 10^{-6}\right) \right]^2 \right\rangle}{d^{2/3}} \tag{50}$$

and assuming that the temperature variations are much smaller than the mean temperature, then

$$\frac{1}{T(r)} \cong \frac{1}{T(r+d)} \cong \frac{1}{T(r)} \cong \frac{1}{T} \quad \text{and} \tag{51}$$

---

[1]Recently, Friehe of Scripps Institute, in a private communication, suggested that humidity variations may contribute significantly to refractive index fluctuations under conditions of high humidity. This has not been generally accepted. It is difficult to measure humidity fluctuations due to a lack of humidiometers that will measure fluctuations with a frequency greater than 15 Hz [25].

$$(52) \quad C_N^2 = \frac{\left\langle \left(79.0 \frac{P}{T^2} \times 10^{-6}\right)^2 [T(r) - T(r+d)]^2 \right\rangle}{d^{2/3}} .$$

Substituting equation (48) into equation (52) gives

$$(53) \quad C_N^2 = \left(79.0 \frac{P}{T^2} \times 10^{-6}\right)^2 (C_T^2) .$$

Thus the analytic expression for C_{NT} is

$$(54) \quad C_{NT} = \left(79.0 \frac{P}{T^2} \times 10^{-6}\right) C_T .$$

In order to calculate C_{NT} using equation (54) measurements of mean pressure, mean temperature and C_T as given in equation (48) must be made. These measurements will be described in the experiment section of this thesis.

IV. EXPERIMENTAL APPARATUS AND PROCEDURES

This section will describe the apparatus and procedures used to make measurements during the project. The specific results and conclusions derived from the measurements will be reported in later sections.

Two major systems were used to measure the data obtained during the three main experiments. The scintillometer system measured the standard deviation of the logarithmic intensity distribution, $C_{\ell I}$, for the transmitted laser beam. These measurements furnished the data for the calculation of C_{NO} from equation (45). The thermosonde system measured the temperature structure constant, C_T, mean temperature, T, and the mean pressure, P. These measurements furnished the data used in the calculation of C_{NT} from equation (54). Additional experiments were performed to measure the intensity stability of the laser, the power spectrum of the scintillation and the degree of truncation of the laser beam by the laser output optics. These experiments verified the scintillometer system's performance and accuracy. The equipment used in the experiments will be subsequently described in this section.

A. THE SCINTILLOMETER SYSTEM

The scintillometer system measured the logarithmic intensity variance of the transmitted laser beam. The main components of the system are illustrated in Figure 1.

A low powered helium-neon laser transmitted a beam to an optical receiver. The receiver detected the incoming beam and generated an electrical voltage proportional to the instantaneous intensity of the beam. This signal was analyzed by the laser scintillometer and recorded on magnetic tape. The standard deviation of the logarithmic intensity of the laser beam was computed by analogue processing methods. This section analyzes in detail the operation of this system.

The laser output and pointing system controlled the spot size and direction of the beam (Figure 2). The laser beam was focused by the first lens to a position near the focal point of the output lens. An adjustable mount was provided to give the output lens two degrees of translational freedom. The spot size was controlled by changing the focal point of the output lens with respect to the fixed focal point of the first lens. During normal operation, the beam was diverged to minimize beam wander effects. A telescope with cross hairs, bore-sighted with the laser, provided an accurate way of aiming the beam. Beam alignment with the target was controlled by elevation and azimuthal adjustment screws. A chopper was provided to interrupt the beam for ten seconds of every minute during which adjustments were made on the background compensator at the receiver.

After transmission through the atmosphere, a portion of the scintillating beam plus background radiation was collected by the input optics in the detector package (Figure 3). The incoming radiation was passed through a 0.63 micrometer

bandpass filter and focused by a lens through two small apertures. The detector package was aligned in such a manner as to pass the laser beam plus background radiation through the first aperture to the first silicon photocell. The second aperture passed only the background signal which was reflected from a small prism to the second photocell. The photocells generated an output voltage proportional to the intensity of the radiation that impinged upon the photosensitive surfaces.

The two signals were then subtracted in a differential amplifier (Figure 4) thus cancelling the background signal and passing only a signal that was linearly proportional to the laser radiation. During operation, the laser beam was interrupted for ten seconds every minute, during which time, the background signals from the two photocells could be electronically adjusted in order to exactly cancel each other.

The scintillation signal (Figure 5) was amplified by a factor of five and then passed through a logarithmic amplifier. The logarithmic amplifier computed the logarithm of the original signal and sent it to a wide band power amplifier. The signal level was multiplied by a factor of ten and recorded on magnetic tape with an F.M. conversion instrumentation tape recorder. The signal was then fed to a multi-channel pulse height analyzer which sampled the signal level periodically. The pulse amplitude was used as a criterion to address one set of 200 analyzer memory channels. These channels counted the number of pulses of a given

voltage level that were accumulated over a variable time period (usually around four minutes). The pulse height analyzer output consisted of a CRT display of the number of pulses of a given signal level as a function of the logarithm of the beam intensity. This corresponded directly to a non-normalized, probability distribution of the logarithm of the laser beam intensity, ln(I). The CRT display was photographed using a polaroid camera and the photographs (example shown in Figure 6) were later analyzed to determine C_{NO}.

To aid in the analysis, a calibration signal generator provided direct current calibration signals at 25, 50, 100 and 200 millivolt levels which were accumulated and stored on a second set of 200 pulse height analyzer channels. The two sets of 200 channels could be displayed in such a manner as to superimpose the calibration signals and the scintillation pulse height distribution. Amplifier and pulse height analyzer memory drift were found to be negligible for the system.

Measurements by Tatarski [1], Ochs [3] and Dowling [4] have shown that the probability distribution of the logarithm of beam intensity is Gaussian. This was expected as a direct result of the central limit theorem and the randomness of atmospheric turbulence. Realizing that the pulse height distribution was Gaussian, then the maximum point corresponded to the mean value of the distribution and the standard deviation of the logarithmic intensity, $C_{\ell I}$, could be measured

directly from the photographs. Realizing that for a Gaussian distribution, the full width at half maximum, $X_{F1/2}$, was related to the standard deviation by

$$C_{\ell I} = 0.425\ X_{F1/2} \tag{56}$$

then the standard deviation could be determined from the following equation.

$$C_{\ell I} = 0.425\ S(X_{F1/2} \text{ in cm}) \tag{57}$$

"S" is a scaling parameter that related the distance along the abcissa in centimeters to the signal value in log-intensity units. S was determined by measuring the distance in centimeters between calibration marks and by applying the relation

$$S = \frac{[\ln(V_2) - \ln(V_1)]}{(X_2 cm - X_1 cm)} \tag{58}$$

$$= \frac{\ln \frac{V_2}{V_1}}{(\Delta X)\ cm}$$

where V is the calibration voltage, X is the distance along the abcissa in centimeters and ΔX is the distance in centimeters between two calibration marks, V_1 and V_2. Once $C_{\ell I}$ was determined, C_N was computed using equation (45).

Implicit in the system computation of $C_{\ell I}$ was the approximation that $\ln\langle I\rangle \cong \langle \ln(I)\rangle$. This approximation

was tested by computing both quantities for typical probability distributions of intensity and comparing the difference. The error introduced for large values of C_{NO} was less than 2% and was correspondingly smaller for lower values of C_{NO}. This error was judged negligible compared to the experimental error involved in measuring C_{NT} and was ignored.

The dynamic range and frequency response of the scintillometer were wide enough to process all scintillation signals without distortion. The logarithmic amplifier had a dynamic range of 80 db and distorted voltage levels from the differential amplifier that were less than one millivolt or greater than ten volts. By choosing an appropriate gain setting, the scintillation signal's mean value at the differential amplifier output terminal was controlled to be approximately 100 mV. All other system components had dynamic ranges greater than 80 db. The minimum signal levels detected during the experiments were around five millivolts while the maximum levels were below one volt. System frequency response was flat from dc to 1.5 KHz. However, the scintillation power spectrum was measured to be negligible beyond 300 Hz and hence, the signal frequency response was undistorted.

B. THE THERMOSONDE SYSTEM

The meteorological equipment used for measuring C_{NT} consisted of a platinum wire thermosonde unit, a barometer,

a thermometer and a psychrometer. The platinum wire thermosonde unit measured the temperature structure function, C_T, by measuring the changes in the difference of resistance between two exposed platinum wires mounted on probes. The resistance of each wire was proportional to the temperature of the wire. The system electronics used analogue processing techniques to compute C_T from the equation

$$C_T^2 = \frac{\langle [T(r) - T(r+d)]^2 \rangle}{d^{2/3}}$$

where the value of "d', the probe separation distance, was constant. This system had a linear frequency response from dc to 1 KHz and a wide dynamic range. The system generated a voltage signal corresponding to C_T^2 which was fed to a strip chart recorder. The thermosonde output was recorded as a function of time.

Mean pressure was recorded as a function of time from a barometer. Mean temperature was read and recorded from a mercury thermometer. Relative humidity was also read and recorded from a psychrometer. C_{NT} was calculated from measurements of C_T, mean temperature and mean pressure using equation (54).

C. SCINTILLOMETER PERFORMANCE VERIFICATION EXPERIMENTS

Three minor experiments were performed in conjunction with the scintillation measurements to determine the scintillation power spectrum, laser output intensity stability and beam truncation by the output optics.

Each experiment was necessary to verify the performance of the scintillometer system.

1. Frequency Response and Dynamic Range

In order to assure that all laser beam signal levels were being accumulated by the pulse height analyzer, the dynamic range and frequency response of the system were tested. The system response to a wide range of input signal levels was found to be logarithmic for signals greater than one millivolt and less than ten volts. Typical log-intensity distributions ranged from approximately 15 to 400 millivolts and all measured distributions were within the system's dynamic range.

Similarly, frequency response tests showed that the system would record and process signals with a frequency range of dc to 1.5 KHz without distortion. It was then necessary to determine the scintillation power spectrum to justify the frequency response of the scintillometer system. An analogue Fourier spectrum analyzer was designed and assembled using a wave analyzer, calibration oscillator and an X-Y plotter (Figure 7).

The FM instrumentation tape recorder fed a measured scintillation signal through a power amplifier to a wave analyzer. The wave analyzer passed the signal through a tunable bandpass filter (bandwidth of 3 Hz) and then generated a voltage equal to the rms value of the filtered signal. The rms voltage signal was recorded as a function

of time on an X-Y plotter. The system output was a graph of the scintillation signal instantaneous relative log-intensity at the specific frequency as a function of time (Figure 8). The graph was then mechanically integrated (using a planimeter) to find the average relative intensity of the signal at the specific frequency. By tuning the bandpass filter to a variety of frequencies and recording the signal intensity, the scintillation intensity power spectrum could be measured.

The tunable bandpass filter had a low frequency cut-off at 20 Hz. The system frequency response was extended to 5 Hz by playing the tape of the scintillation signal at four times the original recording speed and thereby increasing the original signal frequency by a factor of four.

A tunable oscillator was used to calibrate the wave analyzer bandpass filter by generating a pure sinusoidal wave at the desired frequency and tuning the filter to match that frequency. An oscilloscope was used to measure the oscillator's output accurately.

2. Scintillation Spectral Analysis

The scintillation power spectrum was analyzed to verify that the system did not distort the high frequency components of the scintillation signal. Spectrum analysis of three one-minute duration signals was accomplished using the Fourier spectrum analysis system. The three signals analyzed represented the maximum, minimum and average values of C_{NO}, recorded during the first Monterey Bay experiment.

The relative intensities of the various frequency components were averaged to give a representative scintillation spectrum as shown in Graph VIII.

High frequency components above approximately 300 Hz had negligible power levels. The system's high frequency distortion limit was approximately 1500 Hz. This was determined by the tape recorder frequency response. The experiment showed that the high frequency components of the scintillation signal were not distorted by the system electronics.

3. Laser Beam Intensity Profile Analysis

The intensity profile of the laser beam was examined to determine the degree of truncation by the output optics. A scanning photomultiplier was used to measure beam intensity as a function of position in the plane of the output aperture. Intensity profiles were measured with and without the output lens in position and examined for beam truncation by the lens holders.

The intensity scans showed this profile to be essentially Gaussian with negligible truncation. The profiles also indicated that the laser power level varied in time, during the warm-up period. Further analysis of intensity stability was necessary to show that the variations in the radiation received by the scintillometer were due to atmospheric propagation effects and not to internal intensity variations.

4. Laser Power Stability Analysis

Laser intensity variations were monitored and recorded using a photomultiplier tube and strip chart recorder. Measurements of intensity as a function of time were taken in the center and wings of the beam profile. All measurements showed large fluctuations in beam intensity during the warm-up period. These fluctuations were in the form of a periodic modulation that gradually decreased in amplitude and increased in period. Maximum modulation occurred immediately after lasing began. After approximately one hour of operation, the intensity stabilized and the modulation became negligible. However, it was noticed that a 5% modulation could be induced in the beam by blowing air across the laser vents after the laser had reached thermal equilibrium. The cool air created thermal stresses on the laser tube and mirror supports, and caused variations in the optical gain.

Realizing that during the second Monterey Bay experiment, the laser's operating environment continuously subjected the laser to thermal stress from meteorological phenomena, the validity of the data would be in doubt if the internal modulations were large. To test the effects of an outdoor environment on the intensity stability, the laser, photomultiplier and strip chart recorder were assembled on the roof of Spanagel Hall and the experiment was repeated. A short propagation path minimized atmospheric scintillation in the beam.

The laser intensity fluctuations stabilized from 35% modulation when lasing commenced, to approximately 4% modulation after one hour. The level of modulation varied with wind velocity but never exceeded 4%.

Assuming that a 5% modulation was the maximum internal intensity variation encountered during the second Monterey Bay experiment, the magnitude of the perturbation effect on the measured value of C_{NO} was calculated from

$$C_{\ell I}^2 = \left\langle [\ln(I/\langle I\rangle)]^2 \right\rangle \quad \text{where} \tag{59}$$

$$I = I_s + \Delta I_m$$

In the equation, I_s is the instantaneous intensity of the received beam due to scintillation, and ΔI_m was the deviation from the average intensity due to internal perturbations of the laser output intensity. Calculations using equation (59) with values of $\Delta I_m = \pm 0.05 \langle I \rangle$ and a typical probability distribution of I_s showed that the maximum increase in C_{NO} values was 6.4% (computed for a C_{NO} of 2.0×10^{-8} $m^{-1/3}$, calculations showed that the perturbation effect would be less than 2.22%.

These calculations represented the maximum increase in C_{NO} values due to a continuous, random perturbation of $\Delta I_m = \pm 0.05 \langle I \rangle$. In actual conditions, the measured average intensity perturbation was less than 5%. These estimates are an upper bound for possible perturbation effect errors

in the data taken on the second and third of May. The laser was shielded inside a motel room during the first Monterey Bay experiment and perturbation effects should have been negligible. Perturbation effects on the laser used during the San Nicolas Island experiment by the research group from the Naval Missile Center are an unknown quantity.

V. DATA ANALYSIS

The primary goals of the laser propagation research project were:

(1) to develop instrumentation and expertise for measurement of laser beam scintillation and micrometeorological turbulence,

(2) to examine the correlation between micrometeorological atmospheric turbulence and laser beam scintillation and

(3) to verify Tatarski's [1] formulation of the theory of laser propagation through a turbulent atmosphere, in the marine boundary layer.

Three main experiments were performed between January and May of 1973 during which optical and meteorological data were collected. The first experiment was conducted on January 10. The laser radiation was transmitted across Monterey Bay from the Holiday Inn to a receiver in a laboratory at Hopkins Marine Station (see Figure 9). Micrometeorological measurements were made on-board the Naval Postgraduate School's Research Vessel Acania. The second experiment was conducted at San Nicolas Island on March 3. A laser on the Island was aimed at an optical detector mounted on the Acania. An additional set of laser scintillation measurements was made by a research group from the Naval Missile Center, Point Mugu, across Laser Bay on San Nicolas Island (see Figure 10). The third experiment was conducted across Monterey Bay between the Holiday Inn and Hopkins Marine Station on the second and third of May. Micrometeorological measurements were taken on the beach adjacent to the

Holiday Inn. The data collected during the three main experiments will be reported and analyzed in this section. General conclusions based on the results of the three experiments will be presented in the following section.

A. FIRST MONTEREY BAY EXPERIMENT

The first Monterey Bay experiment was carried out on January 10. The laser output and pointing system was placed inside a room in the Monterey Holiday Inn. The beam was transmitted a distance of 4.3 kilometers across the Bay to the receiver located at Hopkins Marine Station. The transmission path was horizontal and approximately six meters above the surface. This path was closely transverse to the prevailing wind direction, and was chosen for this reason and to minimize land effects on turbulence homogeneity. The meteorological data were taken on-board the R.V. Acania which was anchored at approximately the mid point of the laser transmission path. The optical and micrometeorological measurements were taken at the same height above the sea surface.

The optical and meteorological estimates of C_N are listed in Data Table I and are shown as functions of time on Graphs I A and B. Graph II is a scatter plot of the values of C_{NO} plotted against C_{NT}.

The optical measurements of C_N were made in the laboratory by processing the tape recorded scintillation signal. The pulse height analyzer accumulated the signal

probability distribution over consecutive five-minute periods. This corresponded to a five-minute integration of the laser beam scintillation signal. Meteorological data were recorded on magnetic tape and later transferred to a strip chart from which the average values of C_T were measured for five-minute periods. Lack of experience in operating the scintillometer system caused several interruptions in data collection.

The experimental error in the optical measurements of C_{NO} was predominantly due to errors involved in measuring the full width of the pulse height distribution. For values of C_{NO} between 2 and 5 ($X10^{-8} m^{-1/3}$), the standard deviation of the measurements was approximately 5%. Instrumentation error and the error involved in measuring optical wavelength and optical path length were much less than 5%.

The experimental error involved in the meteorological measurements of C_{NT} was predominantly due to inaccuracies in determining the average value of C_T over five-minute intervals from strip chart recordings of the instantaneous measurements of C_T. To complicate this process, the thermosonde unit had high and low scales for different extremes of turbulence. Whenever the scale changed, 30 seconds of data were lost due to system transients. The standard deviation was estimated as approximately 20% for the C_{NT} measurements. Errors involved in measuring pressure and temperature and internal system errors were negligible compared to averaging errors. Experimental error bars are indicated at one point

on each graph. These estimates of experimental error apply to all points on the graph.

In analyzing the data, it is important to realize the fundamental difference between the nature of the meteorological and optical measurements. The meteorological measurements represent the degree of turbulence at only one point along the propagation path. The optical measurements represent the integration of turbulence effects on laser propagation over the total propagation path. The point measurements of turbulence showed greater variations in the values of C_{NT} because localized cells of high turbulence strongly affected the meteorological sensors. The optical measurements did not respond to localized cells of strong turbulence unless the dimensions of those cells were significant compared to the propagation path length. The laser beam scintillation, in effect, averaged the effects of atmospheric turbulence over the entire optical path. This is equivalent to saying that the assumption of homogeneous turbulence is not entirely applicable to distances on the order of several kilometers. Hence, one should analyze the data by comparing the average level of C_{NT} to the optical measurements of C_{NO}.

The data showed a strong correlation between the optical and meteorological values of C_N with the exception of three data regions on Graph I. At approximately 1325, the value of C_{NT} increased to 12.0×10^{-8} meters$^{-1/3}$ but the corresponding value of C_{NO} increased to only 4.36×10^{-8} meters$^{-1/3}$.

Again at approximately 1350, the value of C_{NT} increased to $15.0 \times 10^{-8} m^{-1/3}$ whereas C_{NO} remained steady at $3.25 \times 10^{-8} m^{-1/3}$. Finally, between 1525 and 1630, the values of C_{NT} showed large variations. Corresponding optical data remained relatively constant. The average value of the meteorological data was approximately equal to the optical data.

These deviations between C_{NO} and C_{NT} may have been caused by inhomogeneous turbulence which strongly affected the temperature sensors but was not sufficiently widespread to affect the laser beam propagation. The fact that the average value of C_{NT} (between 1525 and 1630) was approximately equal to the relatively steady value of C_{NO} tended to support this explanation. However, it was also possible that the turbulence was homogeneous and that the optical values of C_N became saturated. Although the saturation effect has been observed in over-land measurements by Ochs in 1969 [3], the cause of saturation has not been clearly understood or explained.

Graph II is a scatter plot of the optical and meteorological measurements of C_N. The two lines drawn on either side of the C_{NO}-C_{NT} equivalence line delineate the region where C_{NO} equals C_{NT} within one standard deviation of experimental error. Sixty-five per cent of the data points are within this region indicating good correlation between measurements of C_{NO} and C_{NT}. The meteorological values were systematically higher than the optical values. This

would be expected in the case of saturation. However, the lack of a well-defined saturation level for optical values precludes a definite conclusion.

This experiment indicated that the optical and meteorological systems that had been developed could measure atmospheric turbulence and, for the prevailing conditions of the experiment, the local thermal fluctuations formed a good predictor of beam behavior.

B. SAN NICOLAS ISLAND EXPERIMENT

The next experiment was conducted over the weekend of March 3 at San Nicolas Island. Laser beam scintillation measurements were taken over a one-kilometer path between San Nicolas Island and the R.V. Acania. This experiment tested the feasibility of making scintillation measurements between the shore and a ship. A helium-neon laser on the island was aimed at a shipboard detector package. Meteorological measurements were made on-board the Acania. Independent measurements of C_{NO} were made by the optical propagation group from the Naval Missile Center, Point Mugu.

The data from this experiment are listed in Data Table II. Graph III shows the measurement of C_N as a function of time.

The problem of keeping the laser beam lined up with the optical receiver proved very difficult. The laser operator aimed the beam at a retro-reflector mounted near the detector and used the reflection for sighting corrections.

A gimballed mount was provided for the detector which could be aligned with the laser beam and thereby reduce the effects of ship motion on the detected beam intensity. This system proved crude and awkward to operate. By making measurements at night, the need for a background compensating photocell was eliminated.

The major problem encountered was that the laser beam could not be pointed at the detector for periods of time longer than five to ten seconds due to ship motion. The detector was moved around in the beam by the roll and pitch of the ship causing a kind of inverse beam wander effect and theoretically increasing the measured values of C_{NO}. Variations in laser beam intensity were due to both scintillation and ship's motion. However, by keeping measurement times very short, the effect of ship motion was minimized and several log-intensity distributions were accumulated. Agreement to within about 40% of optical measurements along the beach line, optical measurements from shore to ship and meteorological measurements on shipboard lead to some confidence in the basic measurement techniques.

This experiment showed, however, that a stabilized optical system was necessary to keep the laser beam and detector aligned. The optical system, as constructed, could not reduce ship motion effects to an acceptable level. It was evident that the system needed to be re-engineered for shipboard use.

C. SECOND MONTEREY BAY EXPERIMENT

The final propagation experiment was conducted on the second and third of May across Monterey Bay. As before, the laser radiation was transmitted from the Holiday Inn to Hopkins Marine Station over a horizontal path, five meters above the sea surface. The optical measurements were taken as previously described for the first Monterey Bay experiment. The meteorological measurements were taken on the beach at the Holiday Inn, where the temperature sensors were positioned approximately two meters below the optical propagation path. The values of C_{NT} were extrapolated for the difference in measurement levels.

1. Data Taken on May 2, 1973

Administrative and technical problems caused many interruptions and delays in data accumulation during the first day of the experiment. Numerous beam alignment adjustments caused the system to be shut down often for realignment. The data collected, especially before 1800, were of questionable accuracy. Graphs IV A and B show the optical and meteorological measurements of C_N plotted as functions of time. The average values of the two graphs are approximately equal, especially for data taken after 1800. The large variations in C_{NO} are due primarily to beam alignment problems.

2. Data Taken on May 3, 1973

The data taken on the second day of the experiment (Graphs IV C, D, E, F, G, H) showed better correlation

between the optical and meteorological estimates of C_N. Between 0830 and 1030, the values of C_{NT} increased and varied rapidly in time. Corresponding measurements of C_{NO} showed a lesser increase and did not reach the high values of C_{NT}. This was probably due to the saturation of C_{NO}. Local cells of strong turbulence could have caused these effects but it was doubtful that isolated cells would have caused sequential increases in a period of two hours.

Assuming that atmospheric turbulence over the propagation path was random, one expects that the number of localized cells of atmospheric turbulence that affect one point on the propagation path during a specific time period to be representative of the number of cells that passed any point along the path during the same time period. There was no reason to expect that localized turbulence would cluster around the thermosonde system. One or two strong increases in C_{NT} during a long period of time could be blamed on isolated localized cells of high turbulence that would have little effect on laser beam scintillation. However, successive, strong increases in C_{NT} during a long period of time could only be due to an overall increase in atmospheric turbulence. These arguments tend to support the saturation explanation for the failure of C_{NO} to correlate with C_{NT}.

From 1200 to 1600, the values of C_{NO} and C_{NT} showed high correlation, while atmospheric turbulence remained relatively steady. At approximately 1630, laser

beam alignment was lost and data collection ceased until 1845. During this time period, the values of C_{NT} showed a gradual decrease. When C_{NO} measurements were re-commenced at 1845, values for C_{NO} and C_{NT} showed a high degree of correlation.

3. Data Correlation

Correlation of C_{NO} with C_{NT} was checked by plotting C_{NO} as a function of C_{NT} in Graph V (A, B, C) and Graph VI (A, B, C, D). Graph V A shows the data measured on the second of May. Sixty-one per cent of all the data points lie within one standard deviation experimental error of the C_{NO}-C_{NT} equivalence line. Experimental error bars have been plotted on only one point but apply for all points. No definite level of saturation was observed. Graphs V, B and C, show the data from the second of May sorted according to the mean wind speed at the time of measurement. No definite trends were noticed. For measurements made when the mean wind was less than seven miles per hour, 66% of all the data points lie within one standard deviation of the C_{NO}-C_{NT} equivalence line. For measurements made when the mean wind was greater than seven miles per hour, 59% of all data points lie within one standard deviation of the C_{NO}-C_{NT} equivalence line. The estimated precision and the quality of the data and the lack of a wide range of wind speeds do not justify any significant conclusions concerning the effect of mean wind velocity on C_N measurements.

Graph VI A is a scatter plot of the C_N measurements made on the third of May. A large reduction in technical problems led to a higher level of confidence in the optical and meteorological data taken on this day. Sixty-three per cent of all data points lie within one standard deviation of the C_{NO}-C_{NT} equivalence line. Graphs VI B, C, and D are scatter plots of C_N measurements sorted according to the mean wind velocity at the time of measurement. For data taken during relatively calm periods (Graph VI B), data point dispersion is very large. Only 23% of all the points lie within one standard deviation experimental error of the equivalence line. The data taken during periods when the wind speed was greater than three but less than six miles per hour (Graph VI, C) show much less dispersion. Seventy-nine per cent of the data points are located within one standard deviation experimental error of the C_{NO}-C_{NT} equivalence line. This trend toward less dispersion with higher wind speed is continued in Graph VI D where data points measured during periods when the wind speed was greater than six miles per hour are plotted. In this case, 93% of all the data points are located within one standard deviation experimental error of the equivalence line. These data indicate that an increase in mean wind speed was accompanied by an increase in the homogeneity of the turbulence and thus, less dispersion of data points on the scatter plots.

VI. GENERAL RESULTS

Empirical data from the Monterey Bay experiment indicate that the optical and micrometeorological measurements of atmospheric turbulence correlated well within experimental tolerances. Graph VII shows that 68% of all measurements of C_{NO} and C_{NT} were within one standard deviation experimental error of the C_{NO}-C_{NT} equivalence line. The San Nicolas Island data were excluded from the statistical analysis because of the unresolved problem of ship motion. These results indicate that it is possible to predict laser beam scintillation at a wavelength of 0.63 micrometers in the marine boundary layer from measurements of mean pressure, mean temperature, and the covariance of the temperature fluctuations.

Some evidence indicates that saturation of C_{NO} measurements may have occurred for values of C_N greater than approximately 5.0×10^{-8} meters$^{-1/3}$. However, the lack of a definite level of saturation in the scatter plots suggests that definite conclusions on this must await additional measurements.

The correlation between the optical and meteorological measurements of the refractive index structure constant increased as the mean wind speed increased. Measurements taken on the second of May were inconclusive due to a lack of range in wind speed values. It was expected that turbulence would become more homogeneous as the mean wind increased.

The theoretical model, from which the relations for C_N were derived, assumed homogeneous turbulence in the horizontal plane. Hence, with an increase in wind speed, turbulence should become more homogeneous and the theoretical model should describe the physical processes more accurately in accordance with the experimental results.

The San Nicolas Island experiment demonstrated the feasibility of making scintillation measurements between the R. V. Acania and a shore station. However, problems in laser alignment due to ship motion indicated that the optical receiver system needed to be redesigned. A stabilized control system is needed to keep the laser beam and detector system aligned.

Finally, the high correlation between the optical and meteorological measurements of the refractive index structure constant indicates that Tatarski's description of electromagnetic propagation is essentially valid in the marine boundary layer at a wavelength of 0.63 micrometers. The validity of the theory appears to improve with increasing wind speeds. Additional experiments are needed to obtain conclusive evidence to support Tatarski's formulation over a wide range of meteorological conditions.

VII. FUTURE RESEARCH SUGGESTIONS

Refractive index structure constant measurements should be made over a wide range of turbulence to determine the possible existence and description of the saturation of optical values. These measurements could further substantiate or refute the existing results of this project.

Project measurements were restricted to a single wavelength and propagation distance. Additional experiments should be made to determine the validity of the theoretical model's predicted dependency on the parameters of wavelength and propagation path length. Experiments could be conducted at various wavelengths using various types of lasers.

Equipment should be designed to shield the laser from fluctuating meteorological conditions and to continuously monitor the laser's output intensity. This would reduce the internal intensity modulation and provide a convenient method of determining beam stability.

Additional thermosonde units should be added to the meteorological instrumentation to obtain a more representative sampling of turbulence along the propagation path. This would reduce the possibility of localized isolated cells of inhomogeneous turbulence giving false indications of total path turbulence. Additional experiments should be conducted to determine if the shore line boundary has a significant effect on the meteorological measurements.

Simultaneous measurements of C_{NT} could be made both on the beach and on-board the Acania and compared for correlation.

A digital system should be assembled for both optical and meteorological data. Digitizing the scintillation and temperature fluctuation signals would greatly reduce the experimental error and provide a direct interface with the Naval Postgraduate School's IBM computer.

Finally, the development of a system to make ship-to-shore measurements of laser beam scintillation would be highly desirable. The system would require some form of stabilized optics to reduce ship motion effects. This would make the system totally portable and measurements could be made almost anywhere on the coast.

VIII. PROJECT CONCLUSIONS

The experimental measurements obtained during this research project suggest the following conclusions:

(1) Systems were developed that made possible simultaneous optical and meteorological measurements of the refractive index structure constant in the marine boundary layer.

(2) Laser beam scintillation at 0.63 micrometers was predicted from meteorological measurements of atmospheric temperature fluctuations, mean pressure and mean temperature.

(3) Tatarski's formulation of electromagnetic propagation [1] was valid for propagation in the marine boundary layer at a wavelength of 0.63 micrometers.

(4) The validity of Tatarski's formulation increases with increasing mean wind speed and subsequent increasing homogeneity of atmospheric turbulence.

(5) More research is needed over a wider range of meteorological conditions to substantiate the generality of the project's conclusions. These measurements would resolve the question of the possible existence and description of a saturation effect on optical scintillation measurements of the refractive index structure constant.

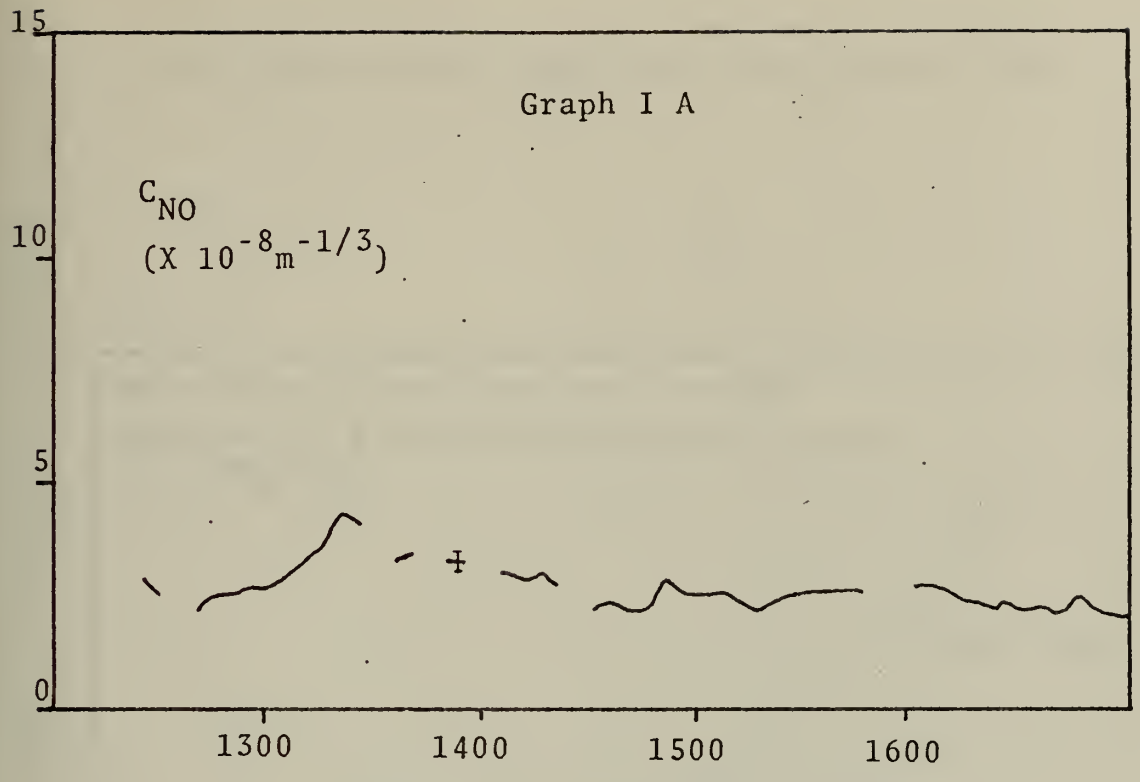

Time Variation of the Refractive Index Structure Constant Measured with the Scintillometer System

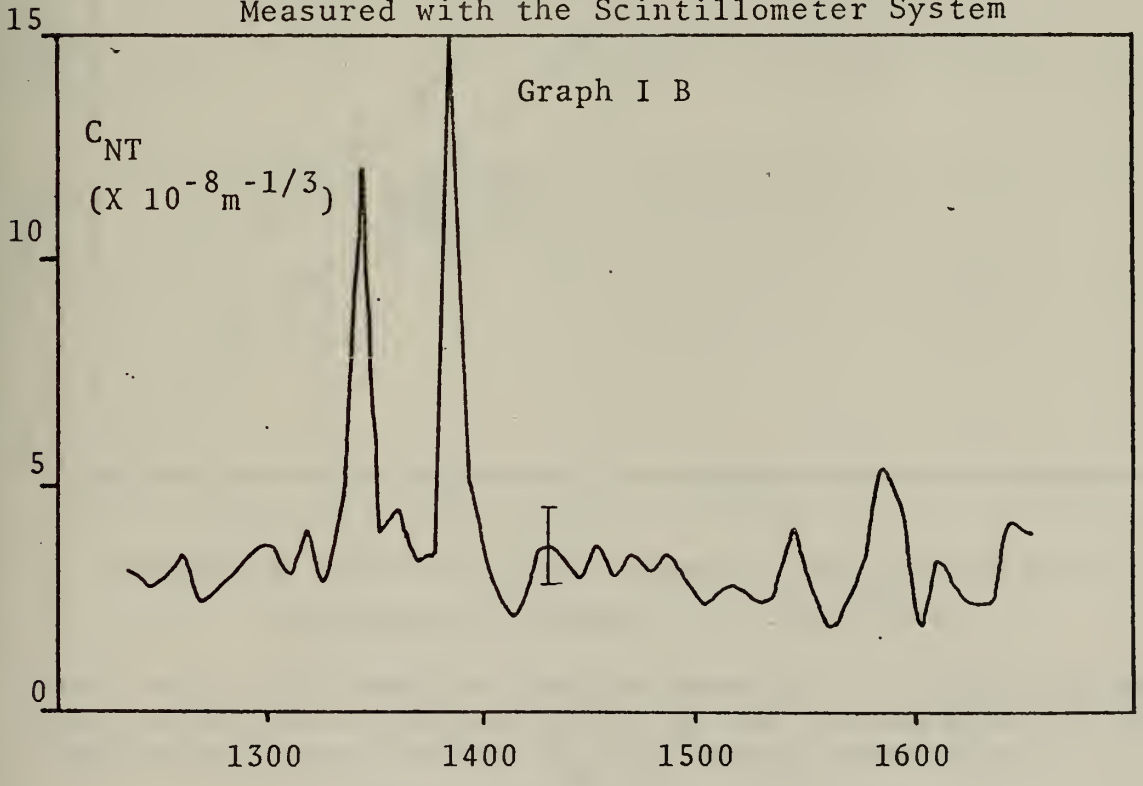

Time Variation of the Refractive Index Structure Constant Measured with the Thermosonde System

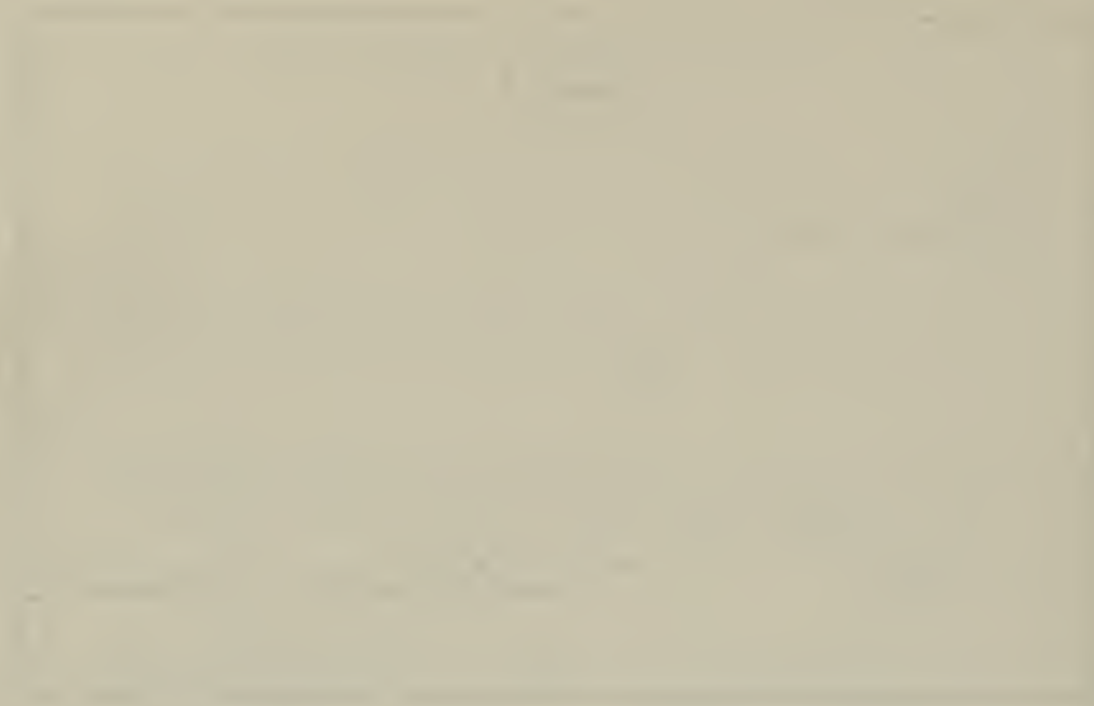

First Monterey Bay Experiment Data Correlation

Graph II

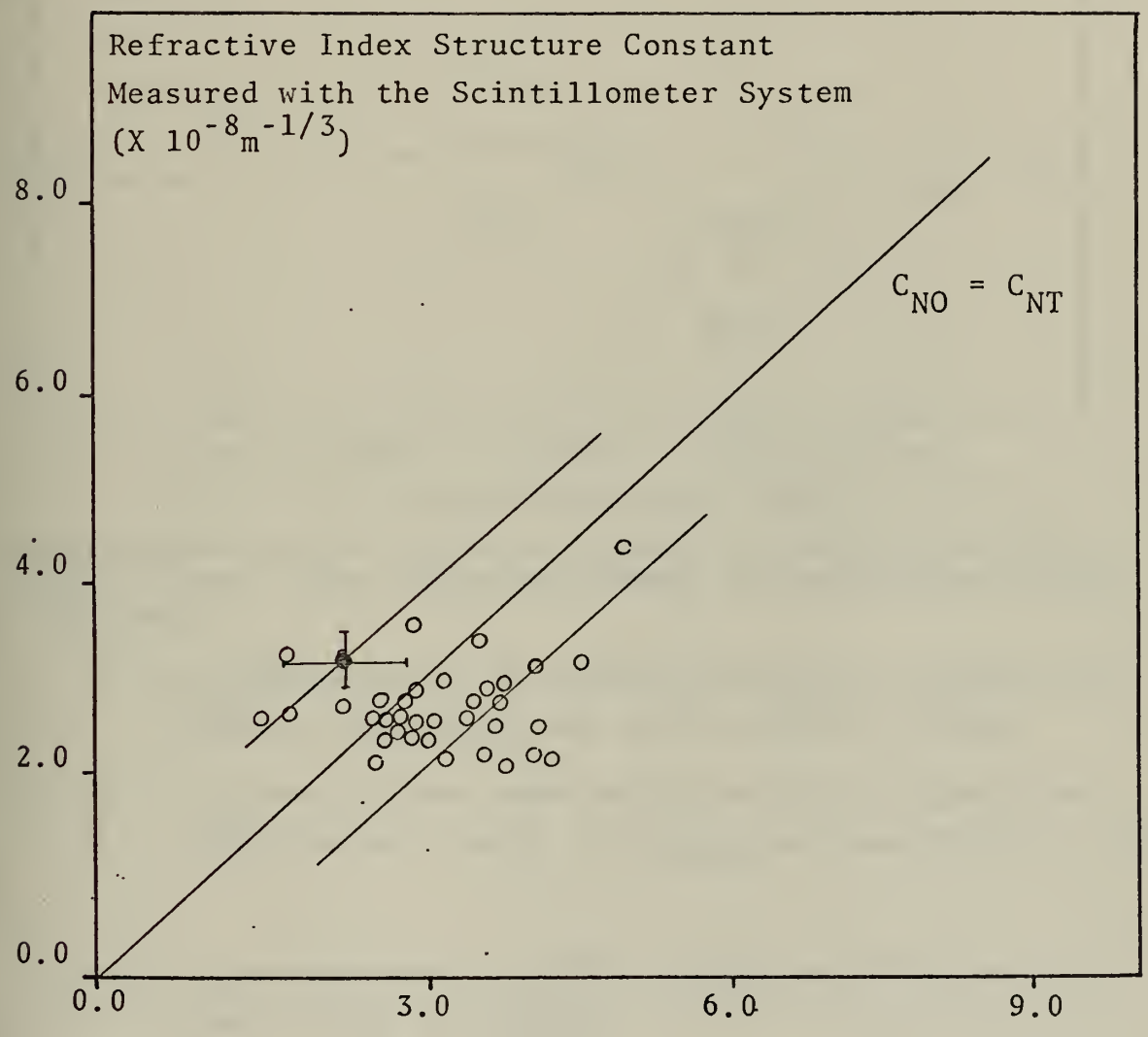

Data taken over Monterey Bay on January 10. Sixty-six per cent of all data points are within one standard deviation experimental error of the C_{NO}-C_{NT} equivalence line.

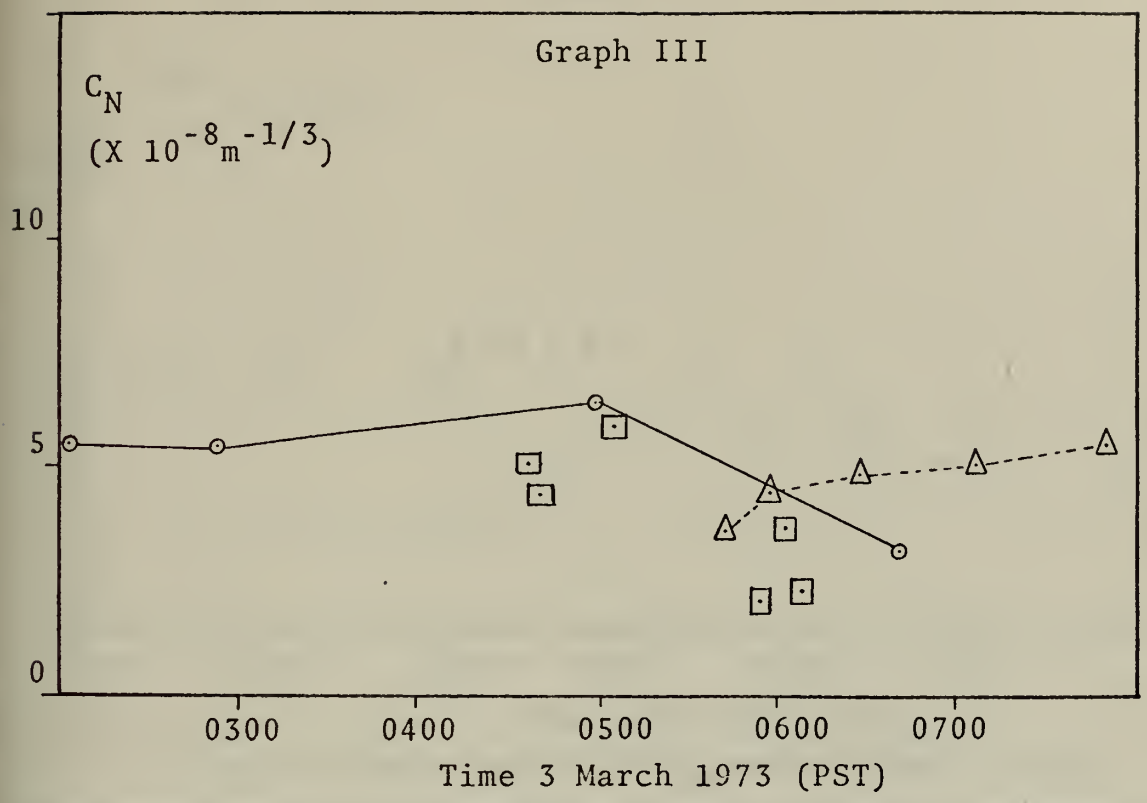

Measurements of the refractive index structure constant versus time. Data collected during the San Nicolas Island Experiment.

⊙ - C_{NO} measurements by NAVMISCEN optical propagation group across Laser Bay on San Nicolas Island.

⊡ - C_{NO} measurements made by NPS optical propagation group between the R. V. Acania and San Nicolas Island.

△ - C_{NT} measurements by NPS meteorological group on-board the R. V. Acania.

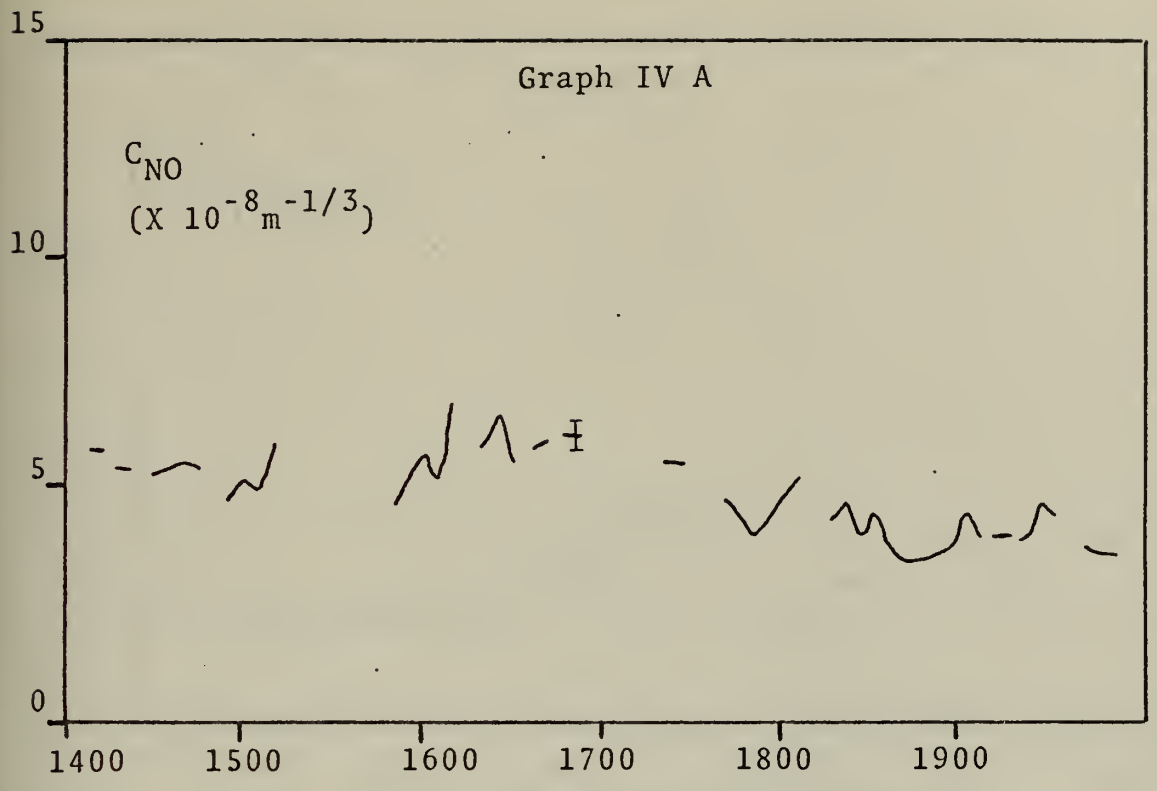

Optical Measurements of C_N versus Time of Day

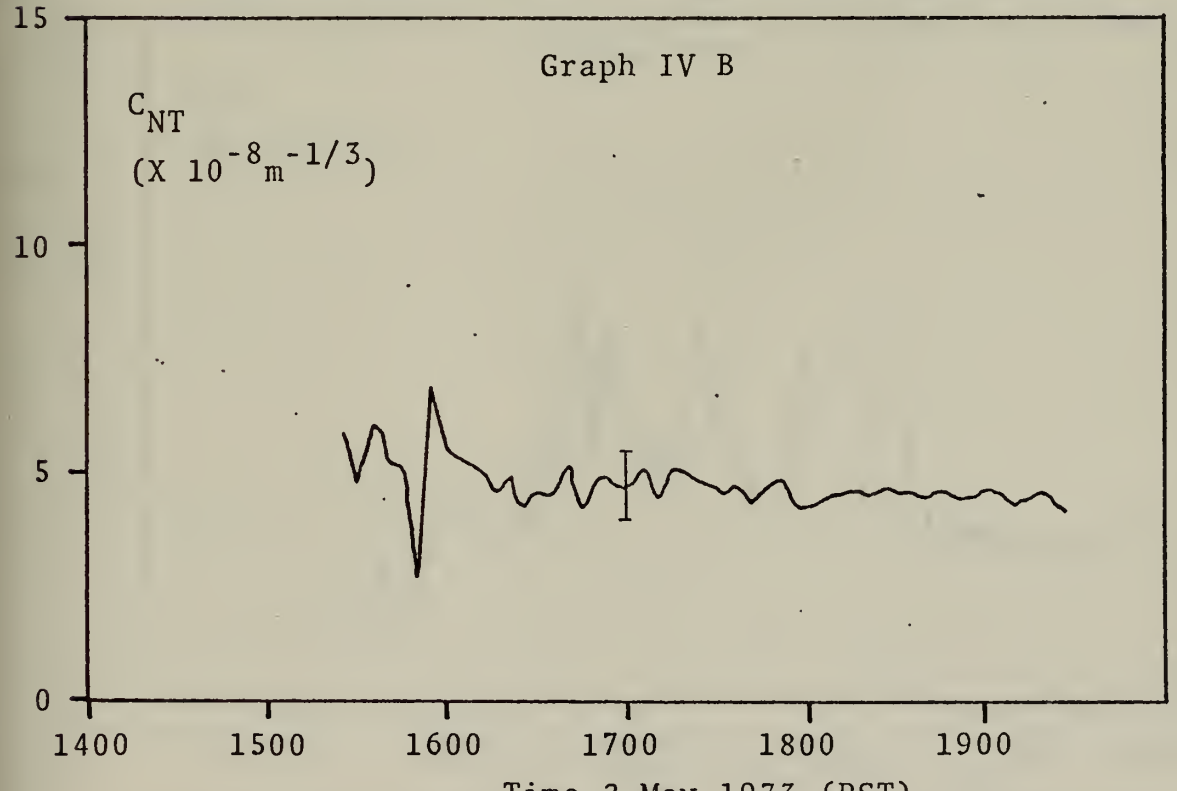

Meteorological Measurements of C_N versus Time of Day.

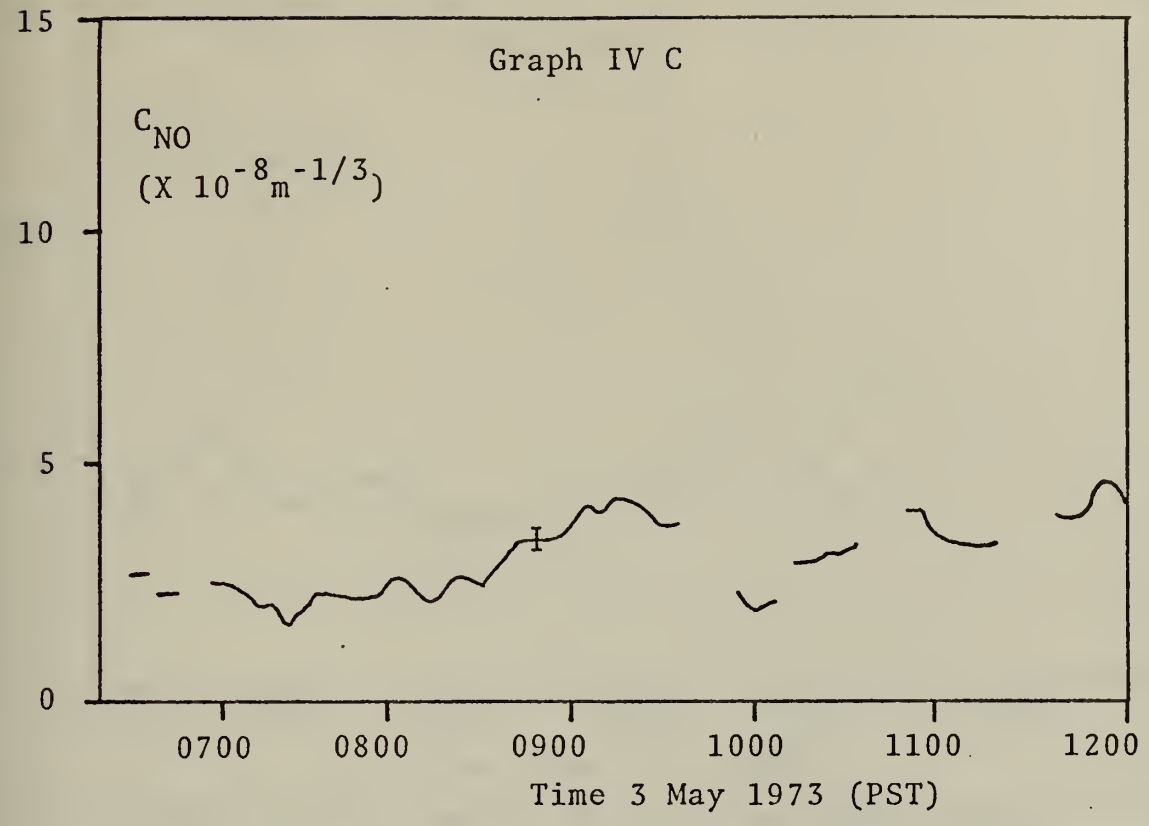

Optical Measurements of C_N versus Time of Day.

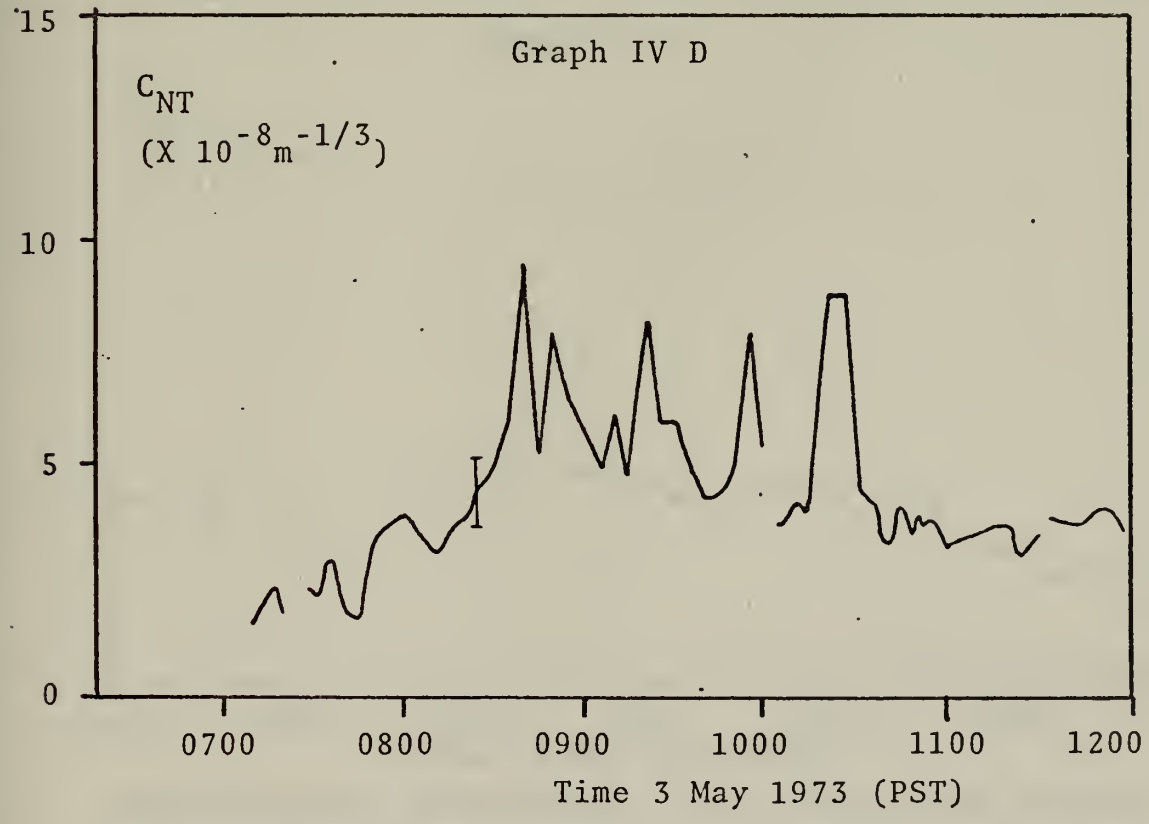

Meteorological Measurements of C_N versus Time of Day.

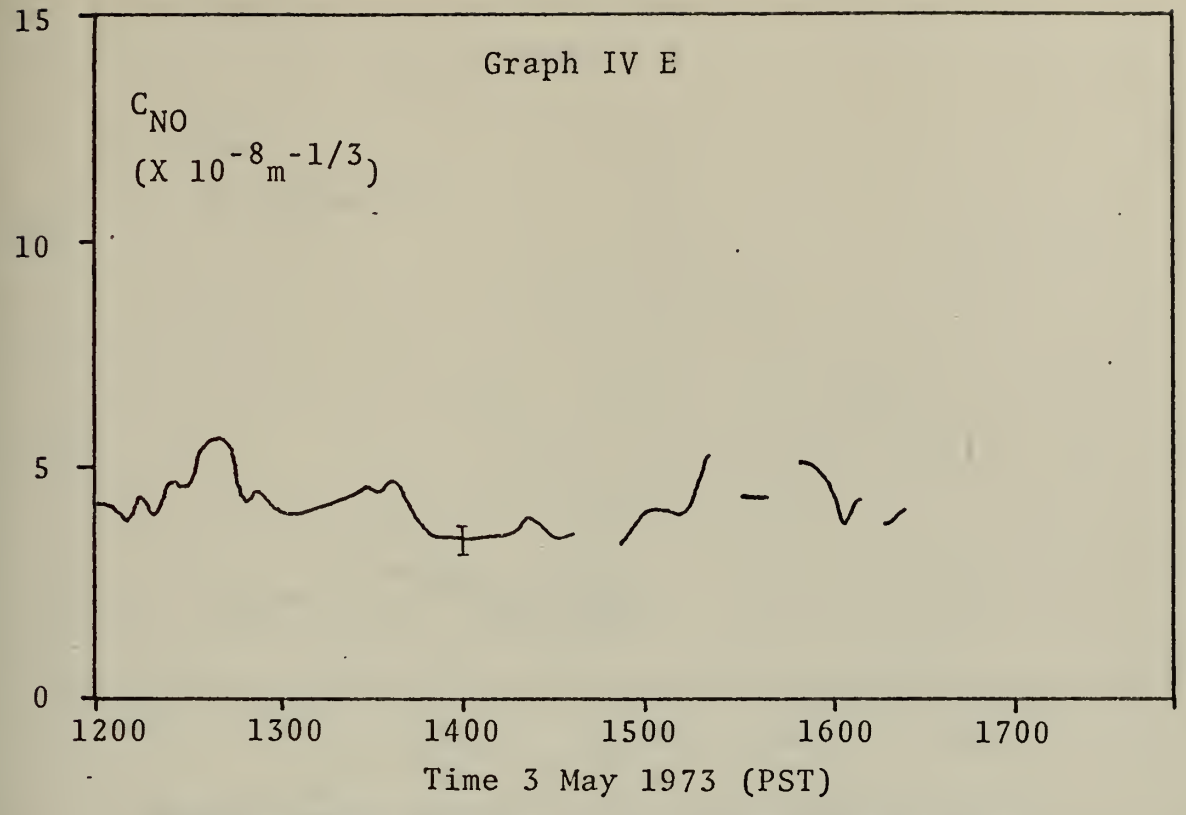

Optical Measurements of C_N versus Time of Day.

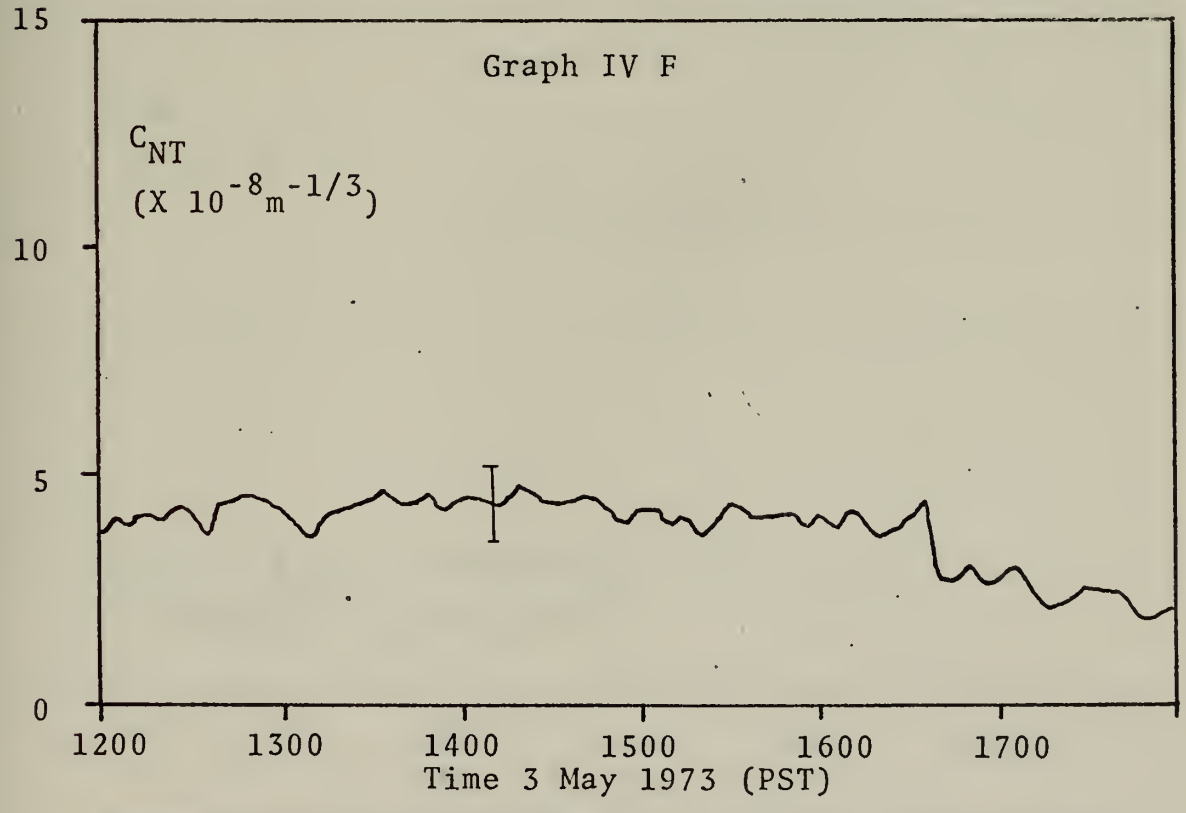

Meteorological Measurements of C_N versus Time of Day.

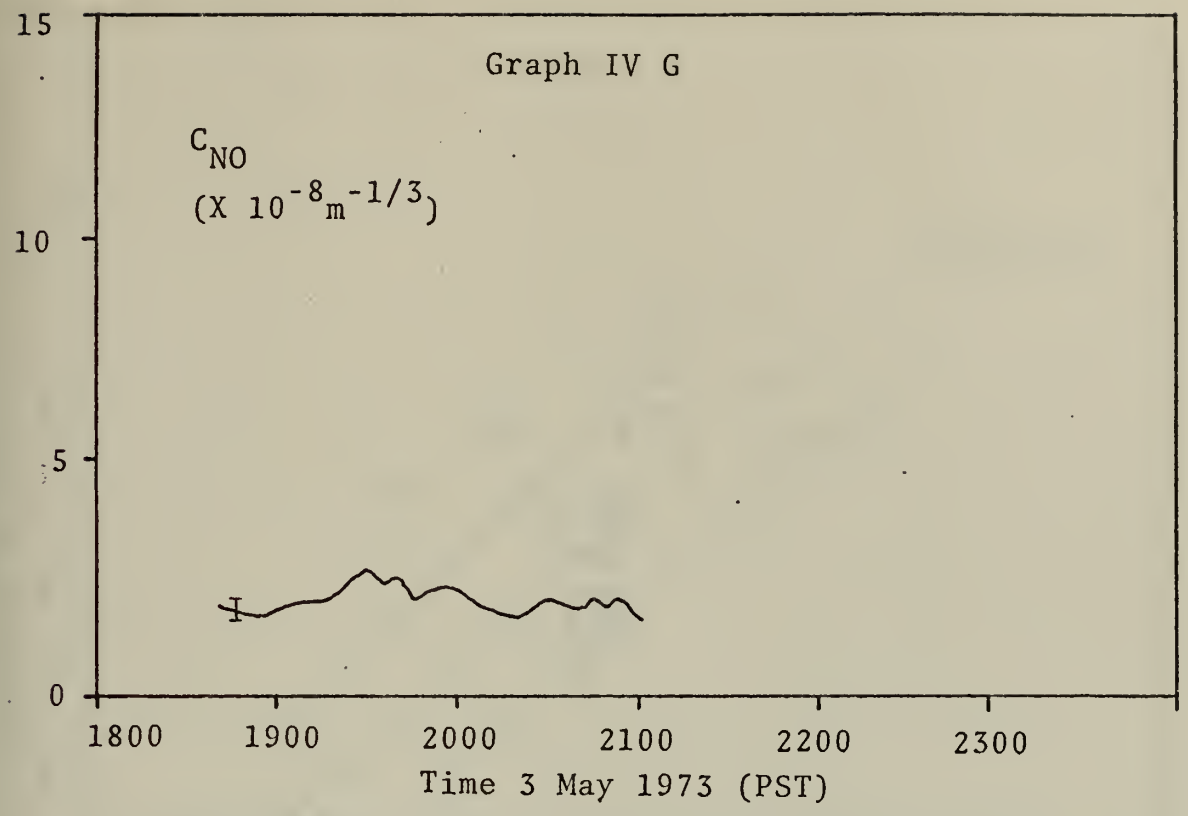

Optical Measurements of C_N versus Time of Day.

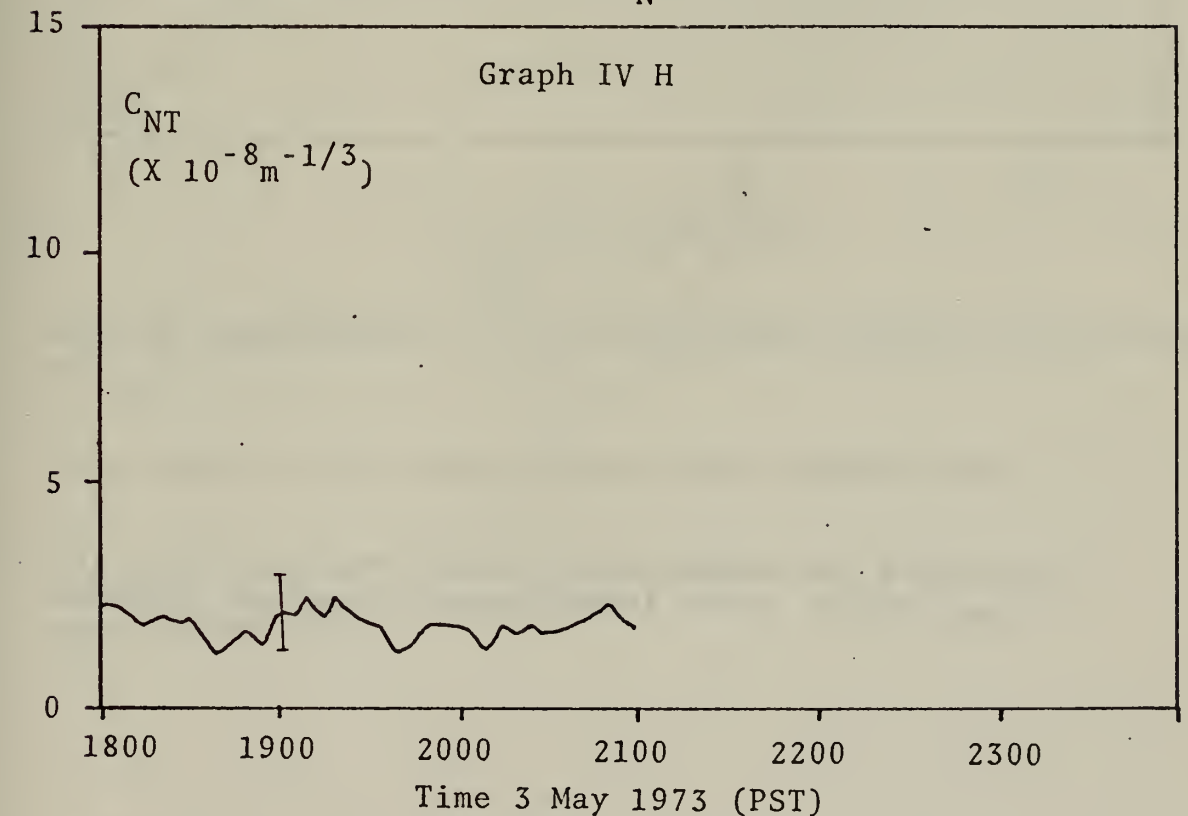

Meteorological Measurements of C_N versus Time of Day.

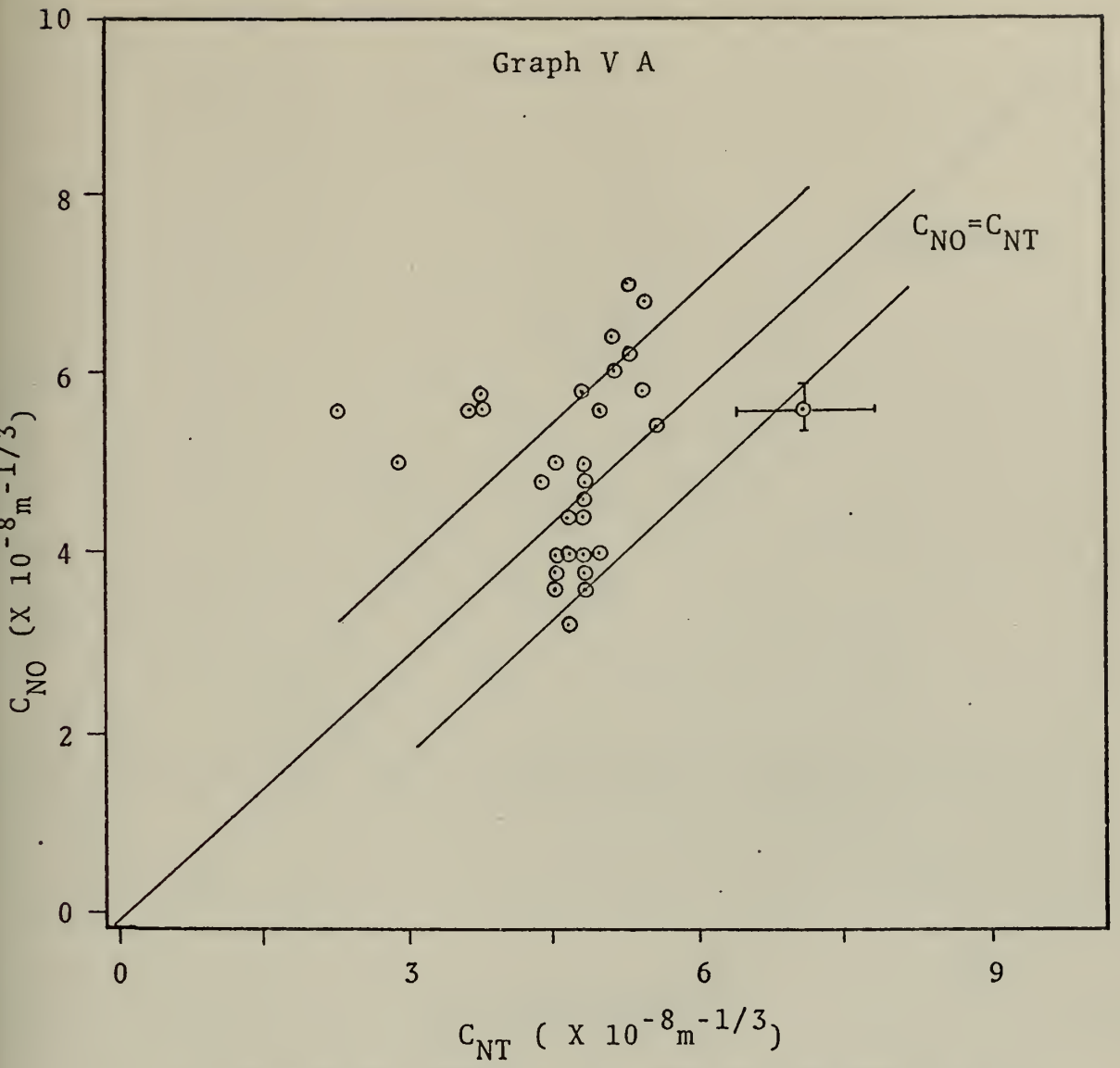

Optical Measurements of C_N versus Meteorological Measurements of C_N.

Data taken on the second of May over Monterey Bay.

Sixty-one per cent of all data points are within one standard deviation experimental error of the C_{NO}-C_{NT} equivalence line.

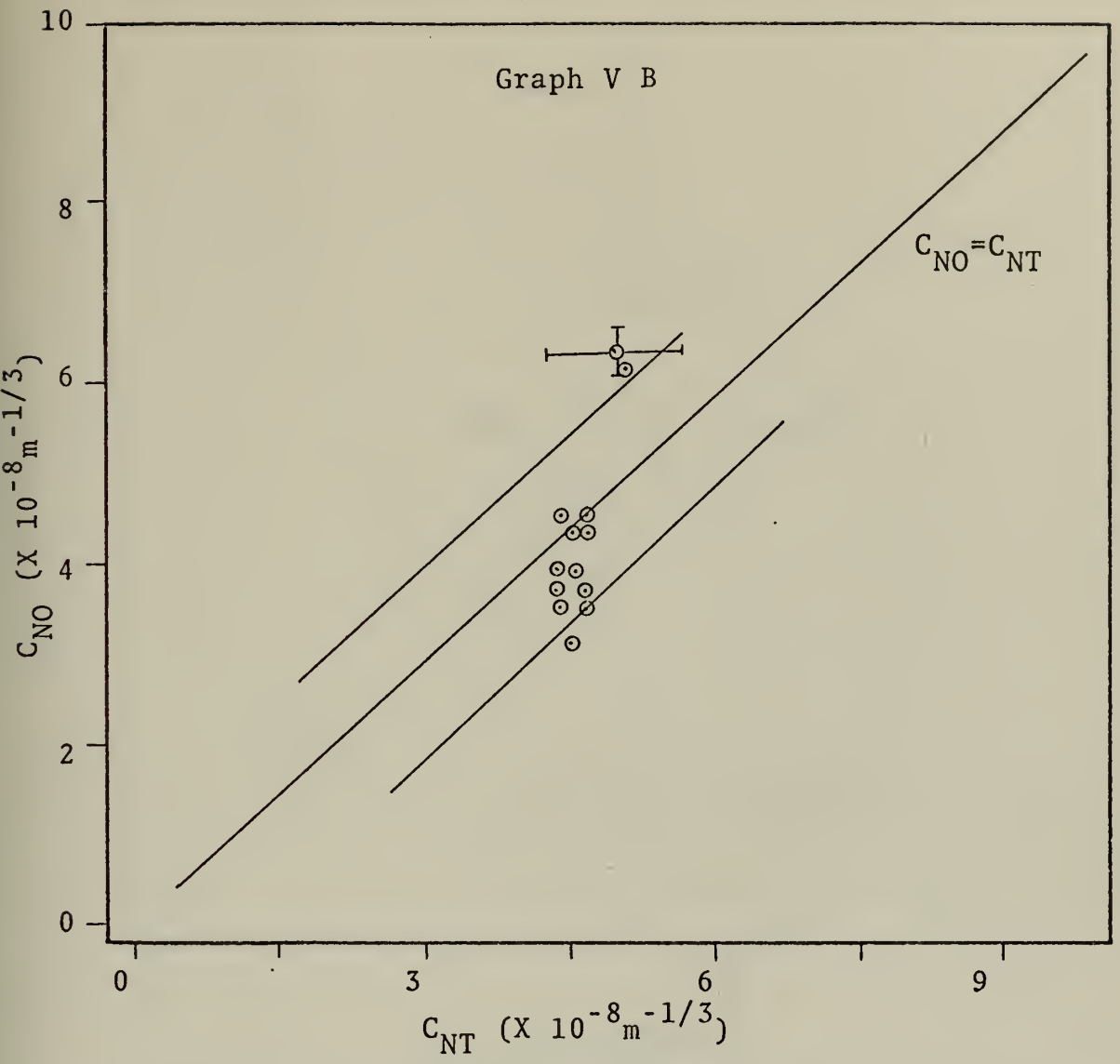

Optical Measurements of C_N versus Meteorological Measurements of C_N. Data Taken when the Mean Wind Speed was less than 7 MPH.

Data taken on the second of May over Monterey Bay.

Sixty-six per cent of all data points are within one standard deviation experimental error of the C_{NO}-C_{NT} equivalence line.

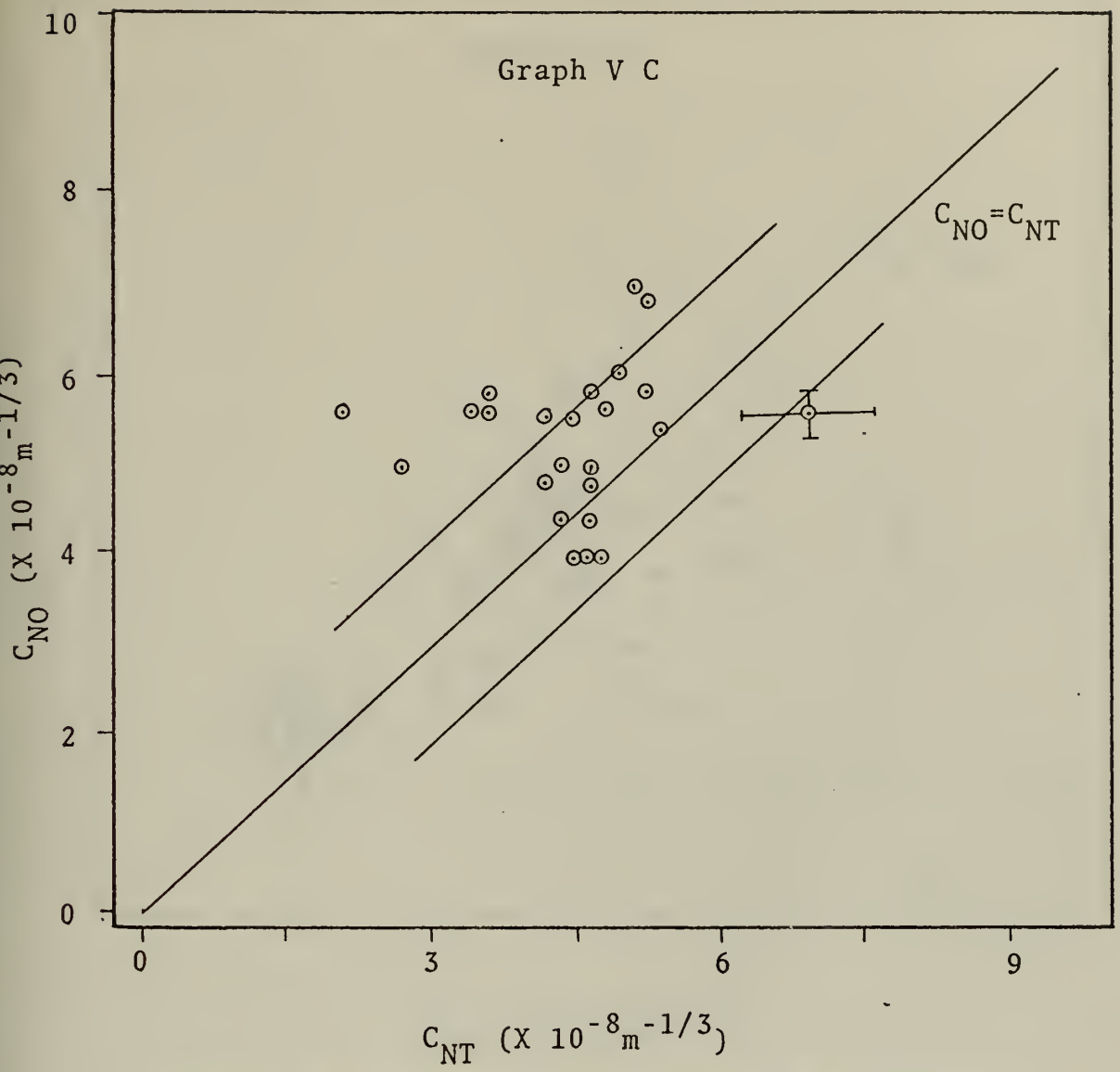

Optical Measurements of C_N versus Meteorological Measurements of C_N. Data Taken when the Mean Wind Speed was greater than 7 MPH.

Data taken on the second of May over Monterey Bay.

Fifty-nine per cent of all data points are within one standard deviation experimental error of the C_{NO}-C_{NT} equivalence line.

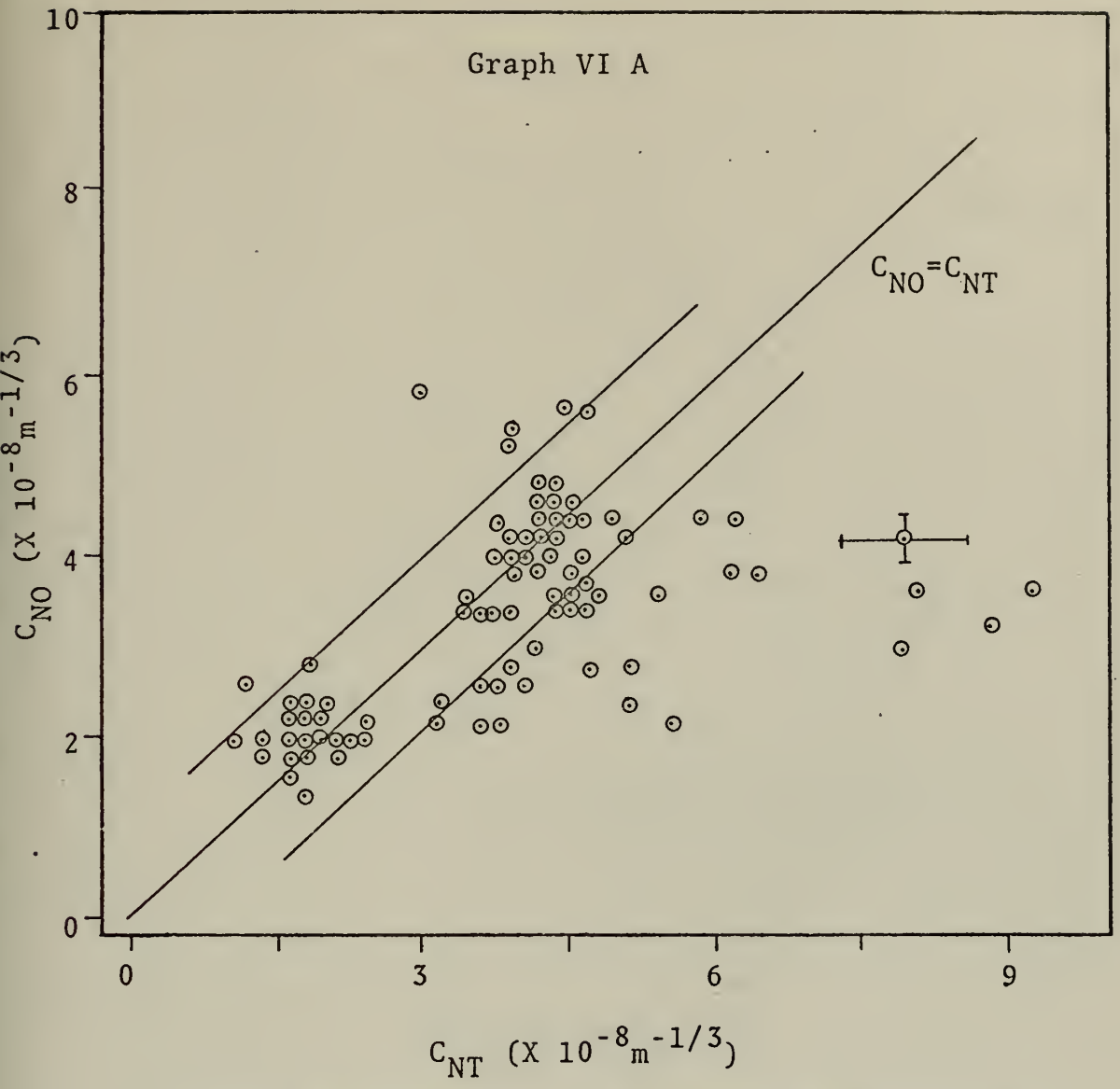

Optical Measurements of C_N versus Meteorological Measurements of C_N.

Data taken on the third of May over Monterey Bay.

Sixty-three per cent of all data points are within one standard deviation experimental error of the C_{NO}-C_{NT} equivalence line.

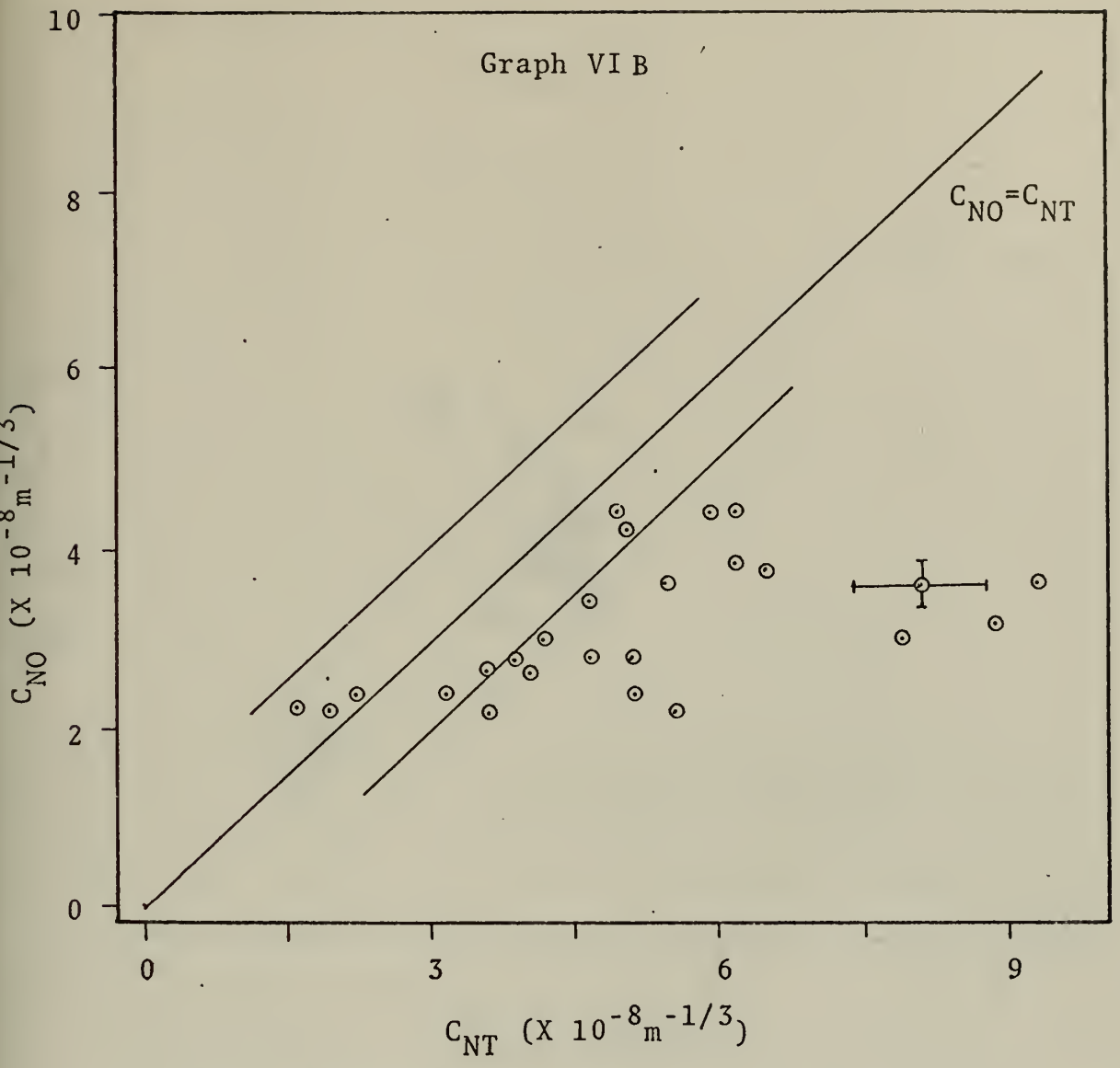

Optical Measurements of C_N versus Meteorological Measurements of C_N. Data taken when the mean wind speed was less than 3 MPH.

Data taken over Monterey Bay on the third of May.

Twenty-three per cent of all data points are within one standard deviation experimental error of the C_{NO}-C_{NT} equivalence line.

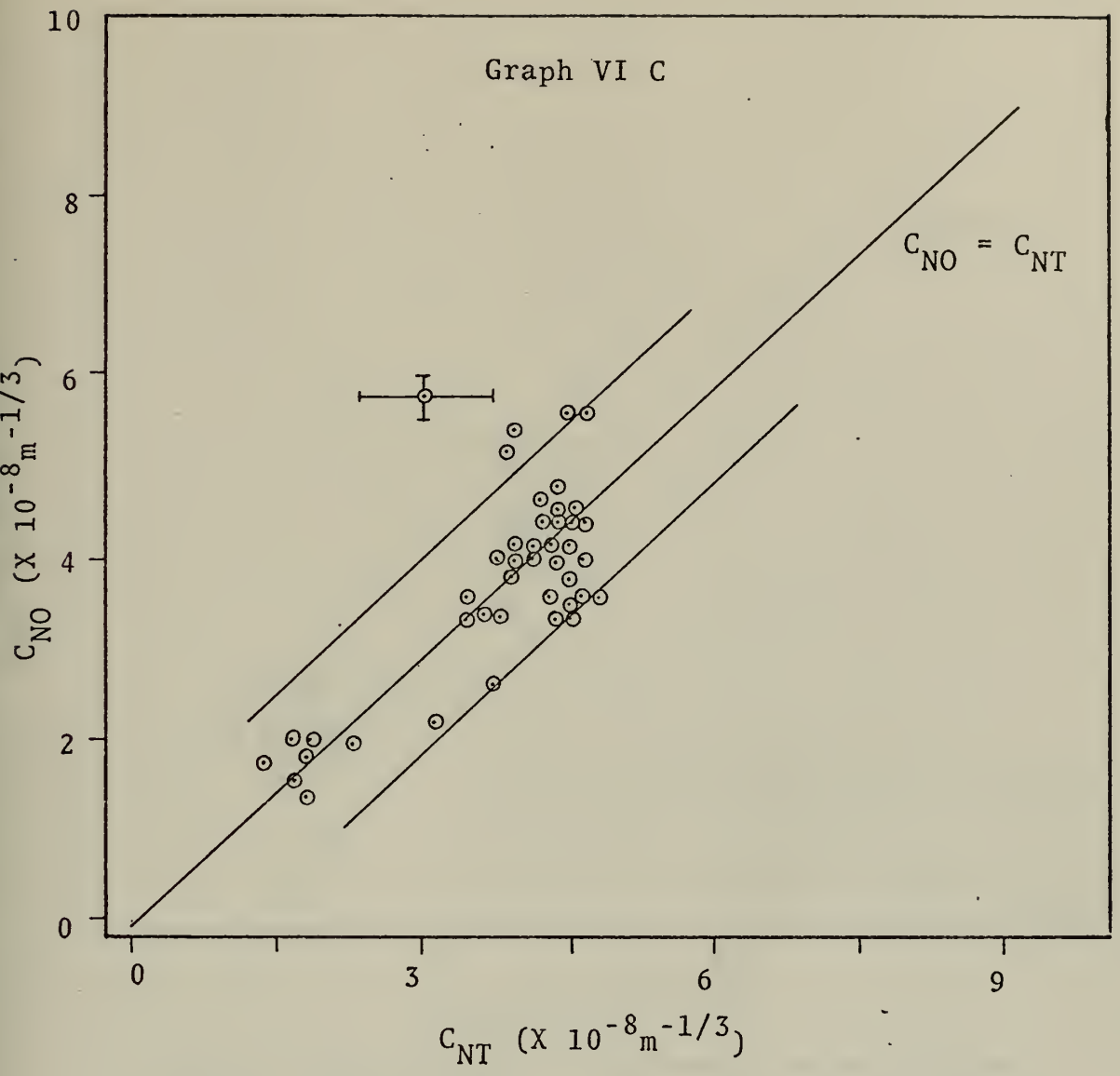

Optical Measurements of C_N versus Meteorological Measurements of C_N.

Data taken when the mean wind speed was greater than 3 MPH but less than 6 MPH.

Data taken over Monterey Bay on the third of May.

Seventy-nine per cent of all data points are within one standard deviation experimental error of the C_{NO}-C_{NT} equivalence line.

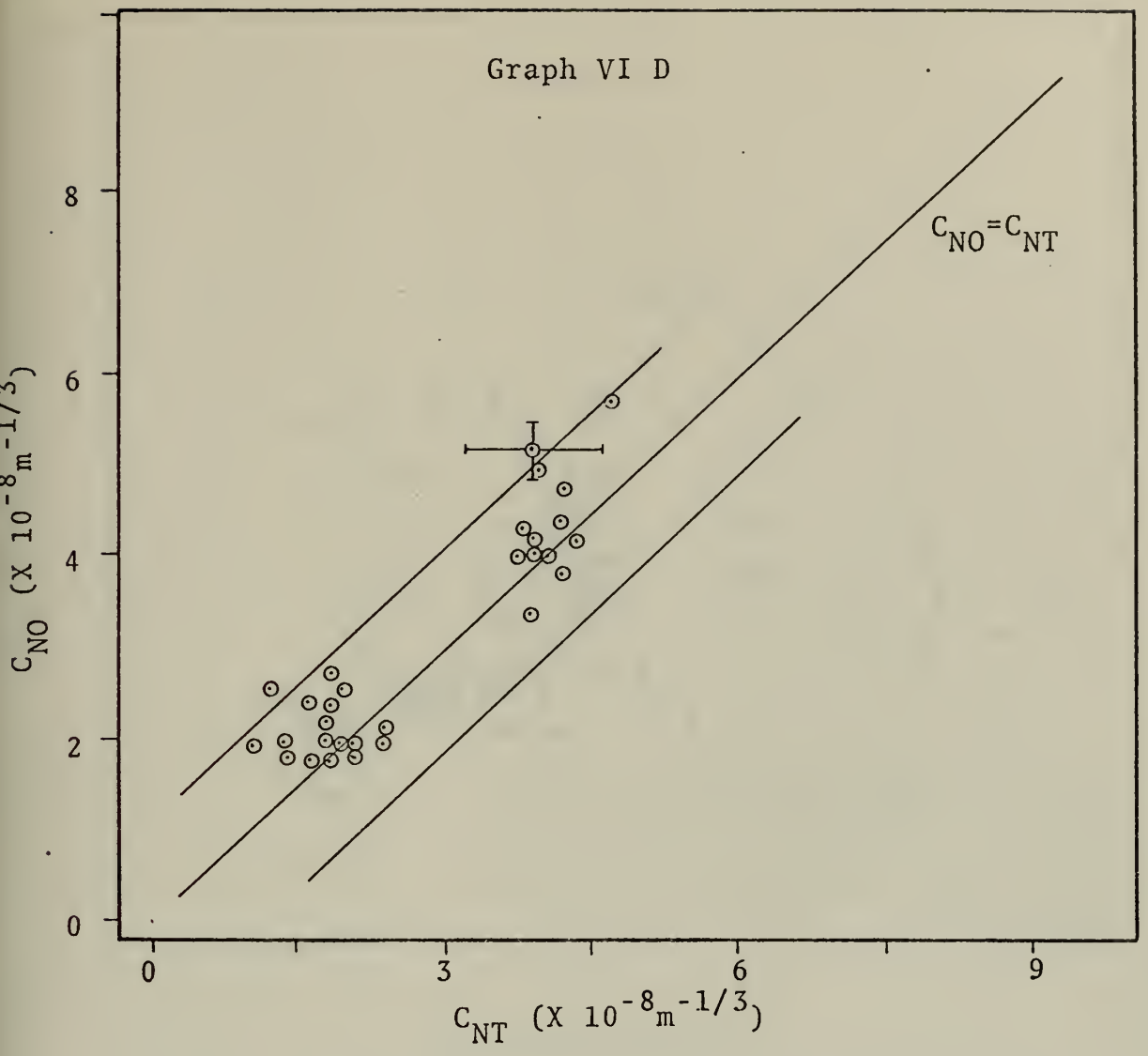

Optical Measurements of C_N versus Meteorological Measurements of C_N.

Data taken when the mean wind speed was greater than 6 MPH.

Data taken over Monterey Bay on the third of May.

Ninety-three per cent of all data points are within one standard deviation experimental error of the C_{NO}-C_{NT} equivalence line.

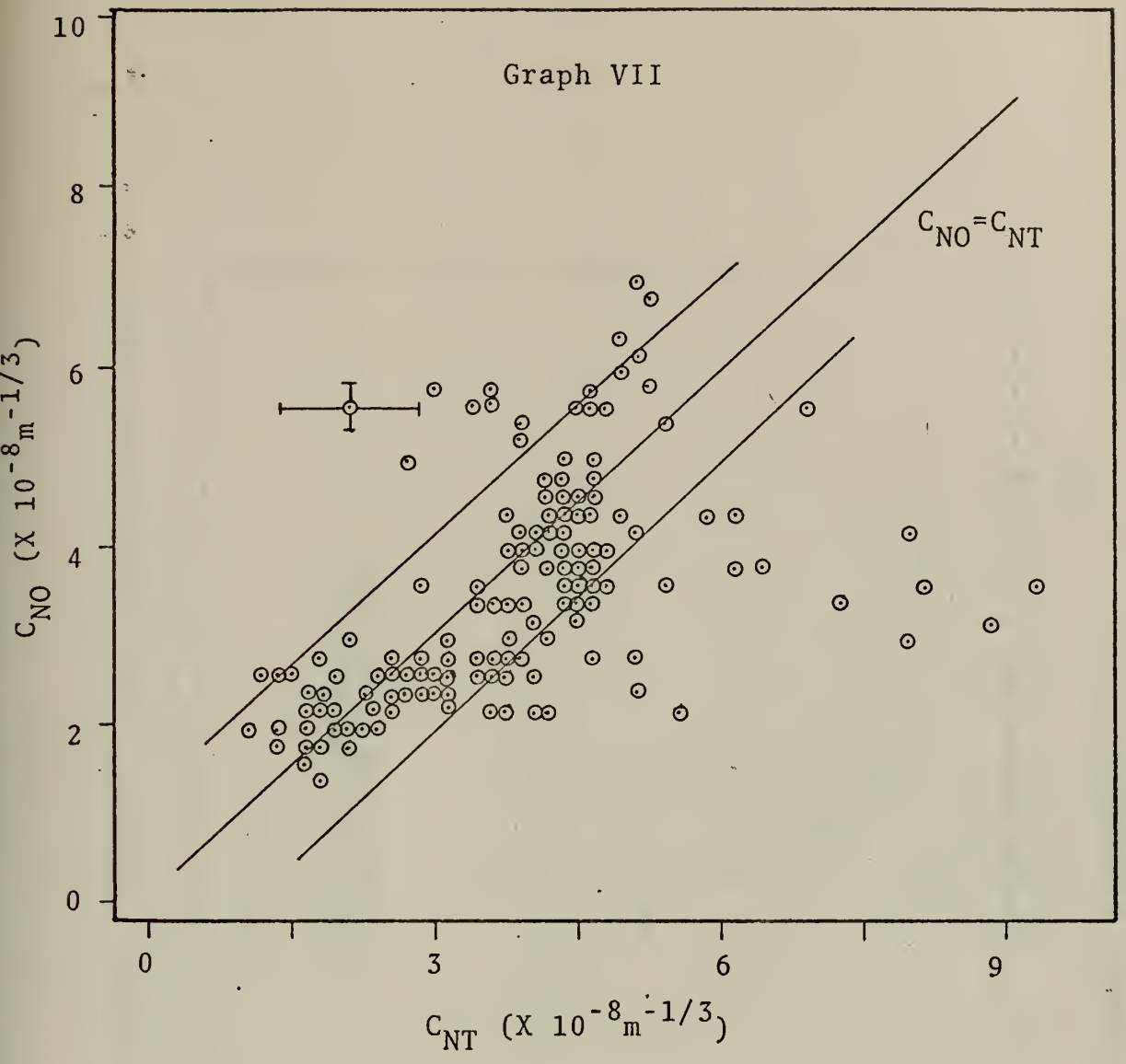

Optical Measurements of C_N versus Meteorological Measurements of C_N.

Includes all measurements of C_N made over Monterey Bay. Excludes San Nicolas Island measurements.

Sixty-eight per cent of all data points are within one standard deviation experimental error of the C_{NO}-C_{NT} equivalence line.

The Frequency Spectrum of the Scintillation Signal

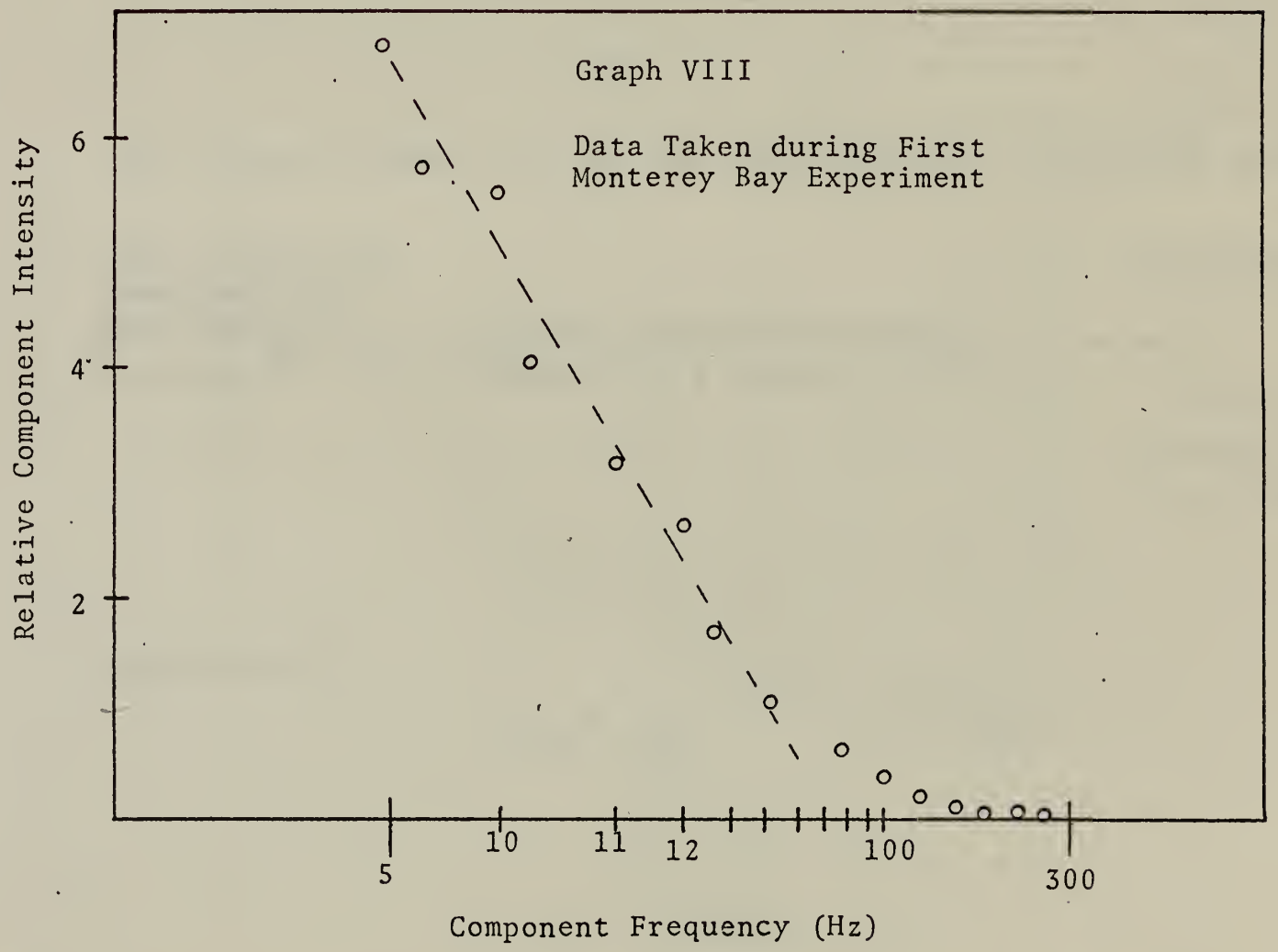

THE LASER SCINTILLOMETER SYSTEM

This system provided the data for the calculation of C_{NO} from equation (45)

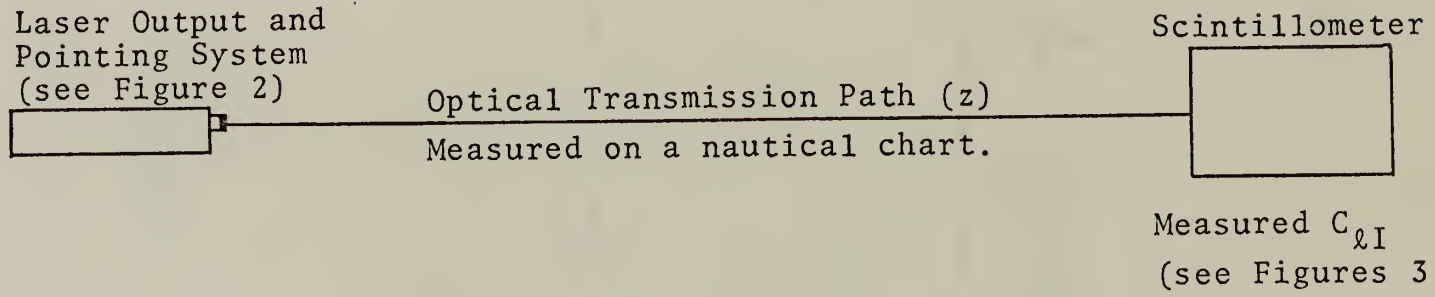

Equation (45)

$$C_{NO} = 1.42\ k^{-7/12}\ z^{-11/12}\ C_{\ell I}$$

Figure 1

LASER OUTPUT AND POINTING SYSTEM

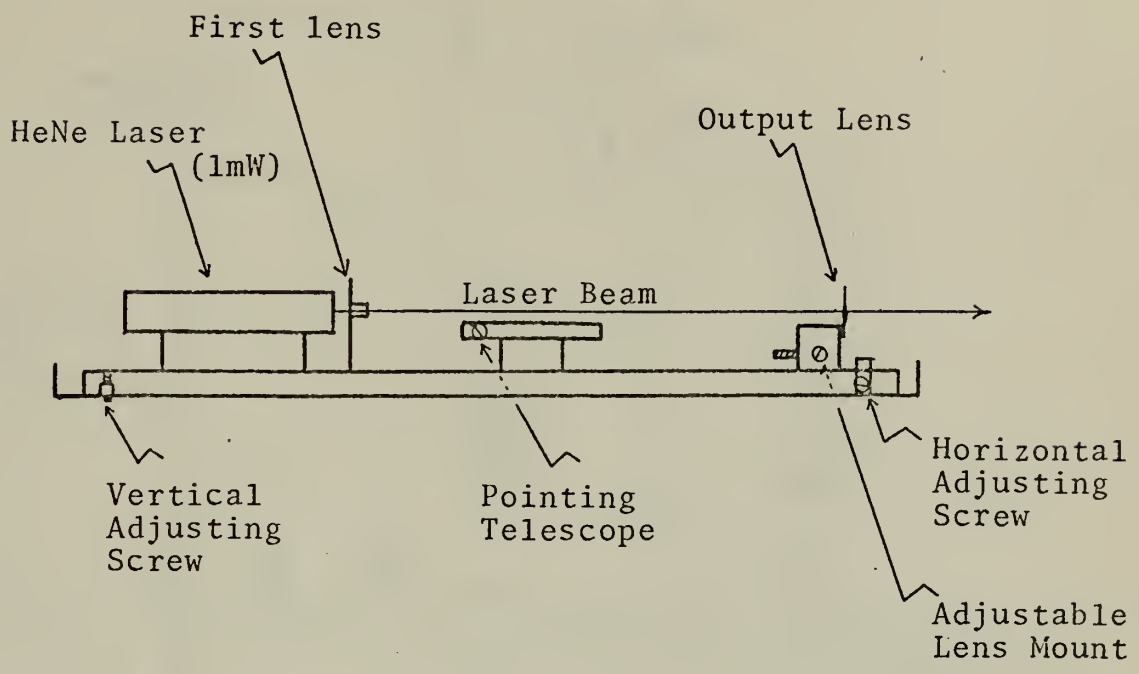

This system was secured to a heavy metal table for vibration isolation.

Figure 2.

OPTICAL DETECTOR PACKAGE

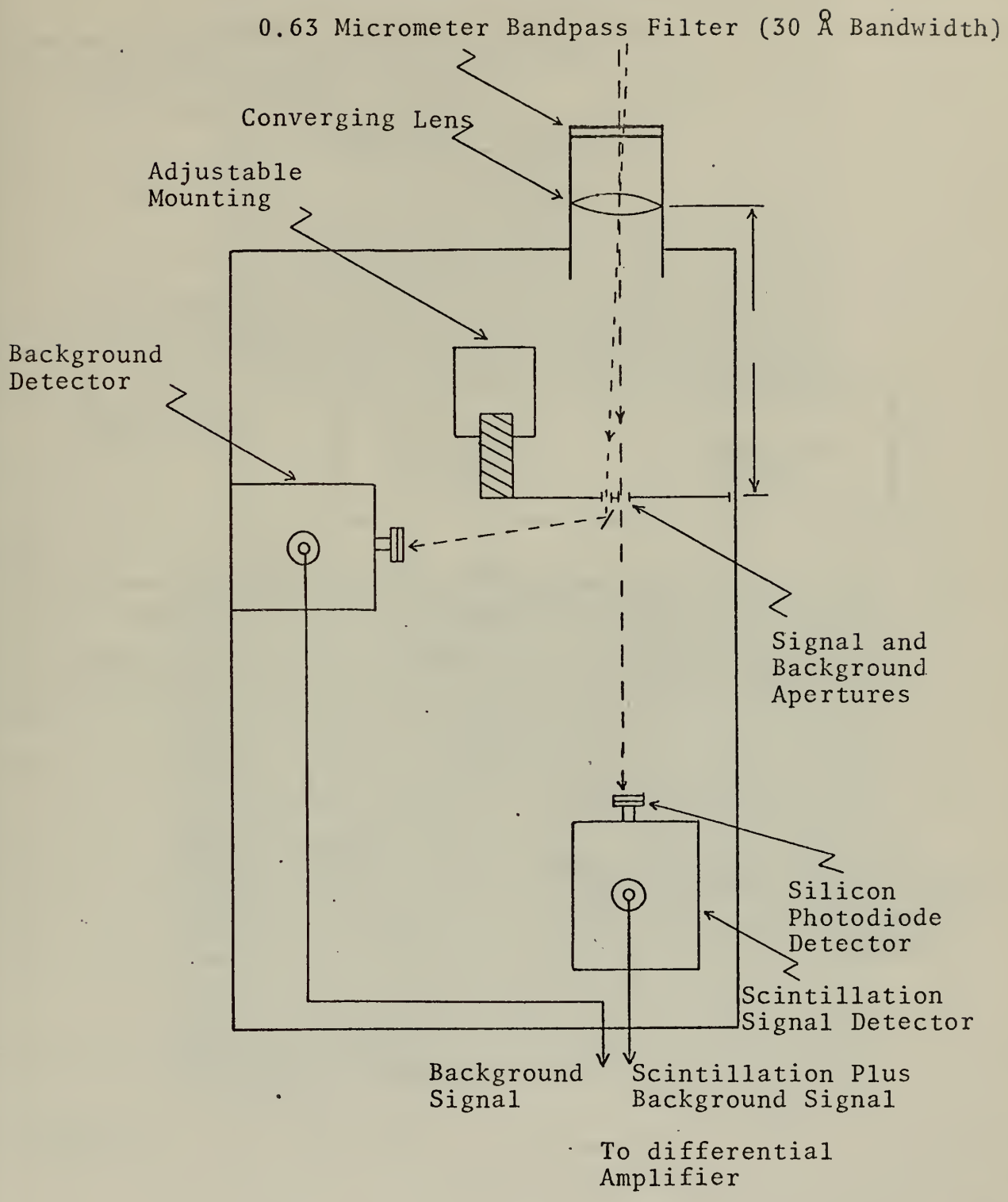

Figure 3.

THE LASER SCINTILLOMETER

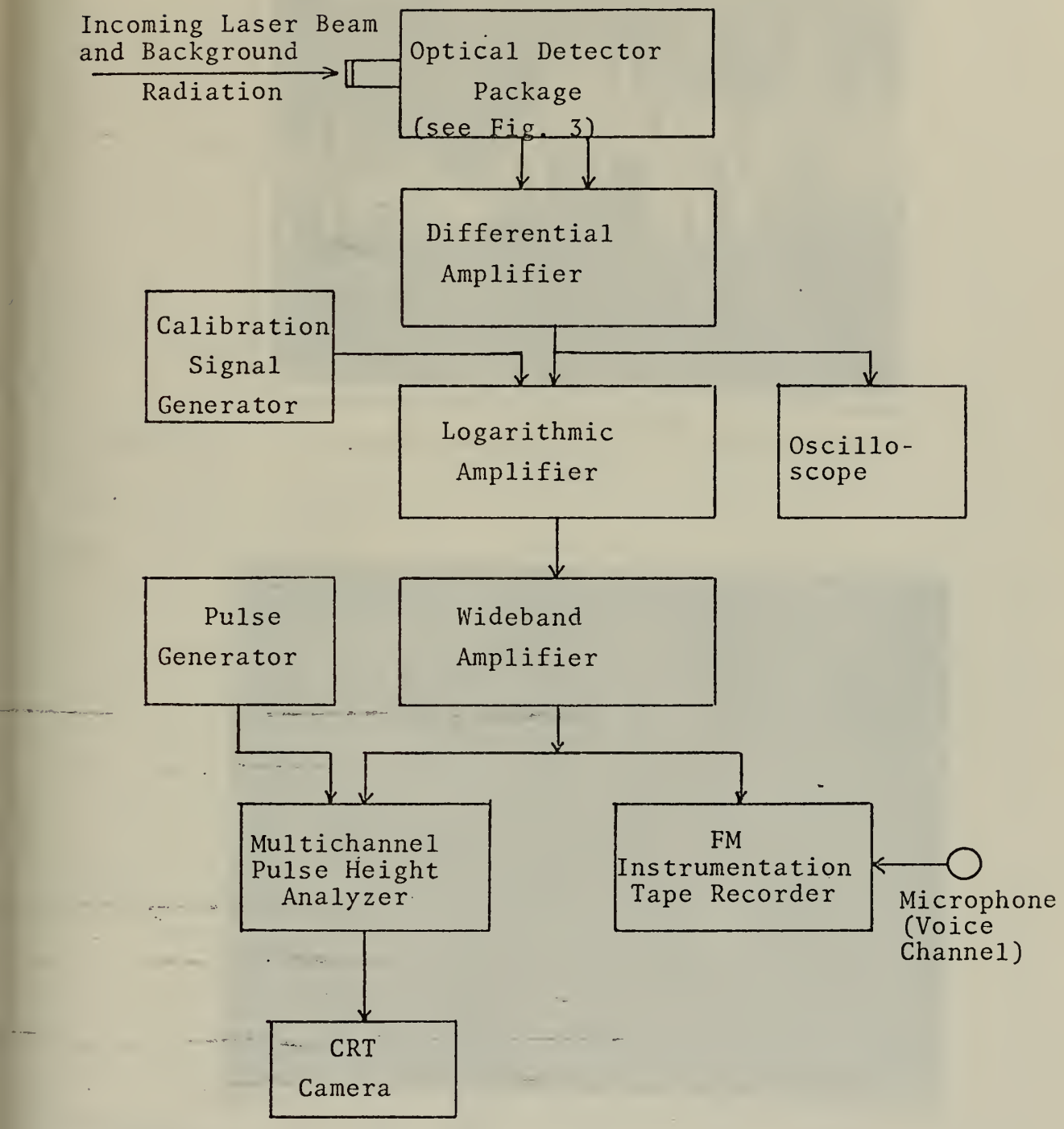

Figure 4.

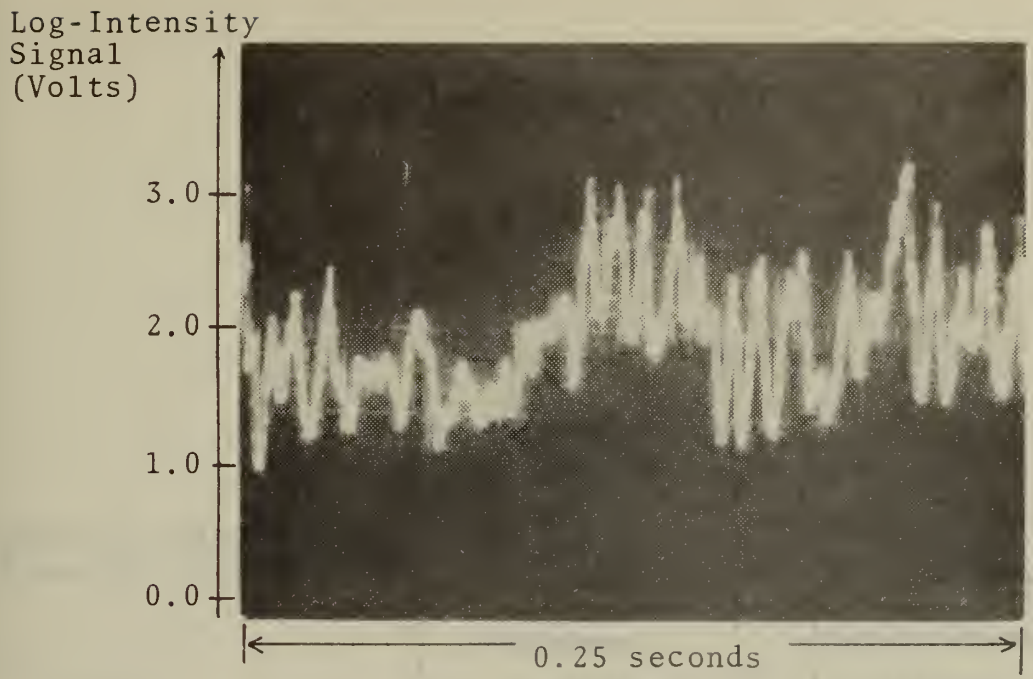

Figure 5. Oscilloscope Trace of the Scintillation Signal

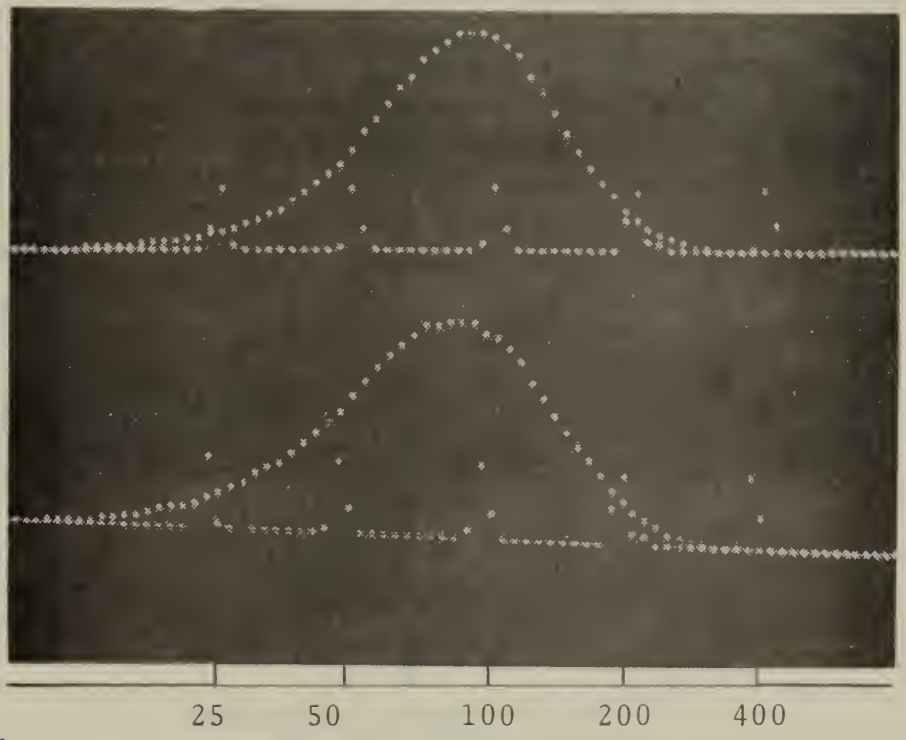

Figure 6. Multichannel Pulse Height Analyzer CRT Display of the Probability Distribution of the Log-Intensity of the Laser Beam.

SCINTILLATION SPECTRUM ANALYZER

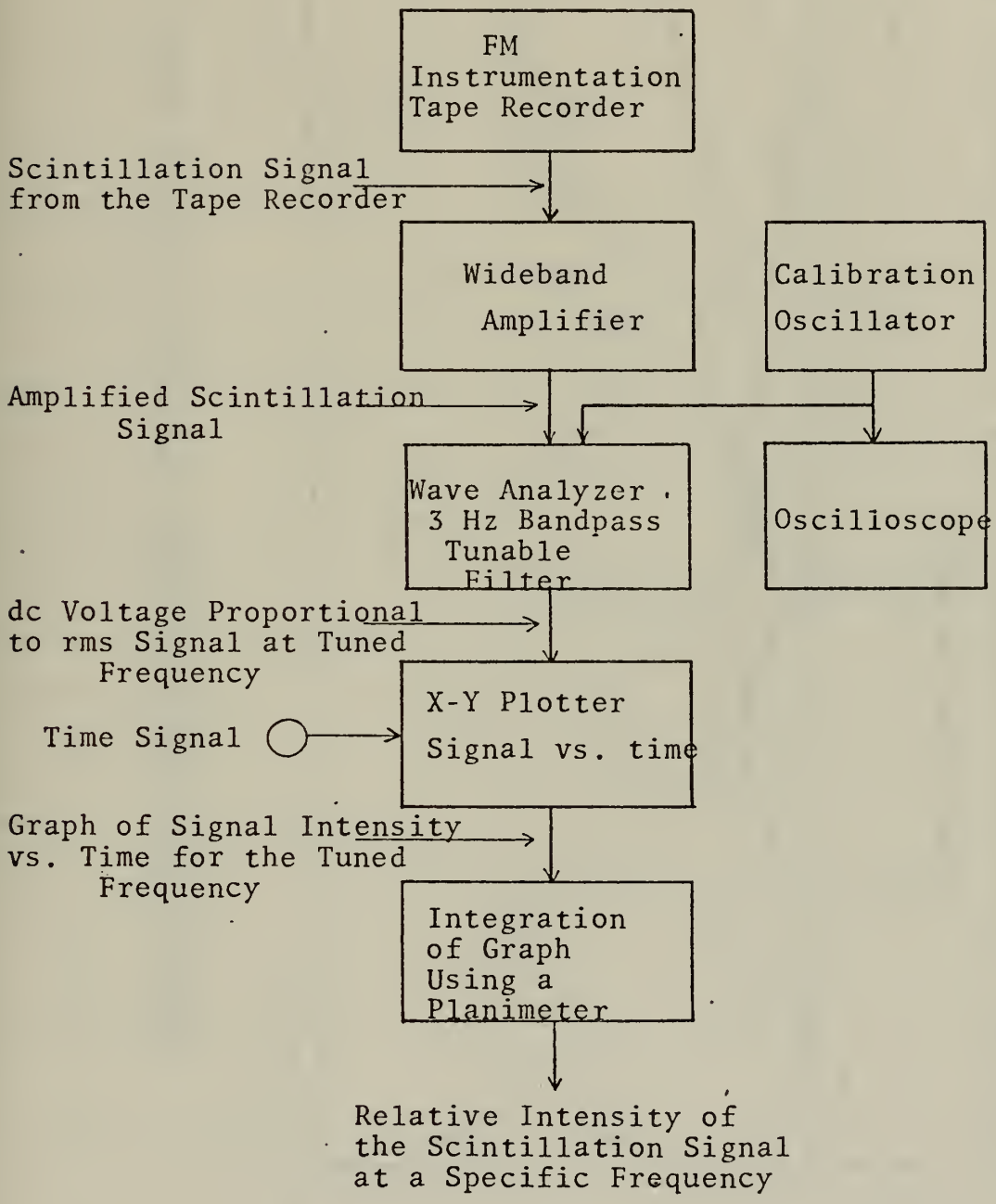

Figure 7.

SCINTILLATION SIGNAL FREQUENCY COMPONENT INTENSITY VERSUS TIME

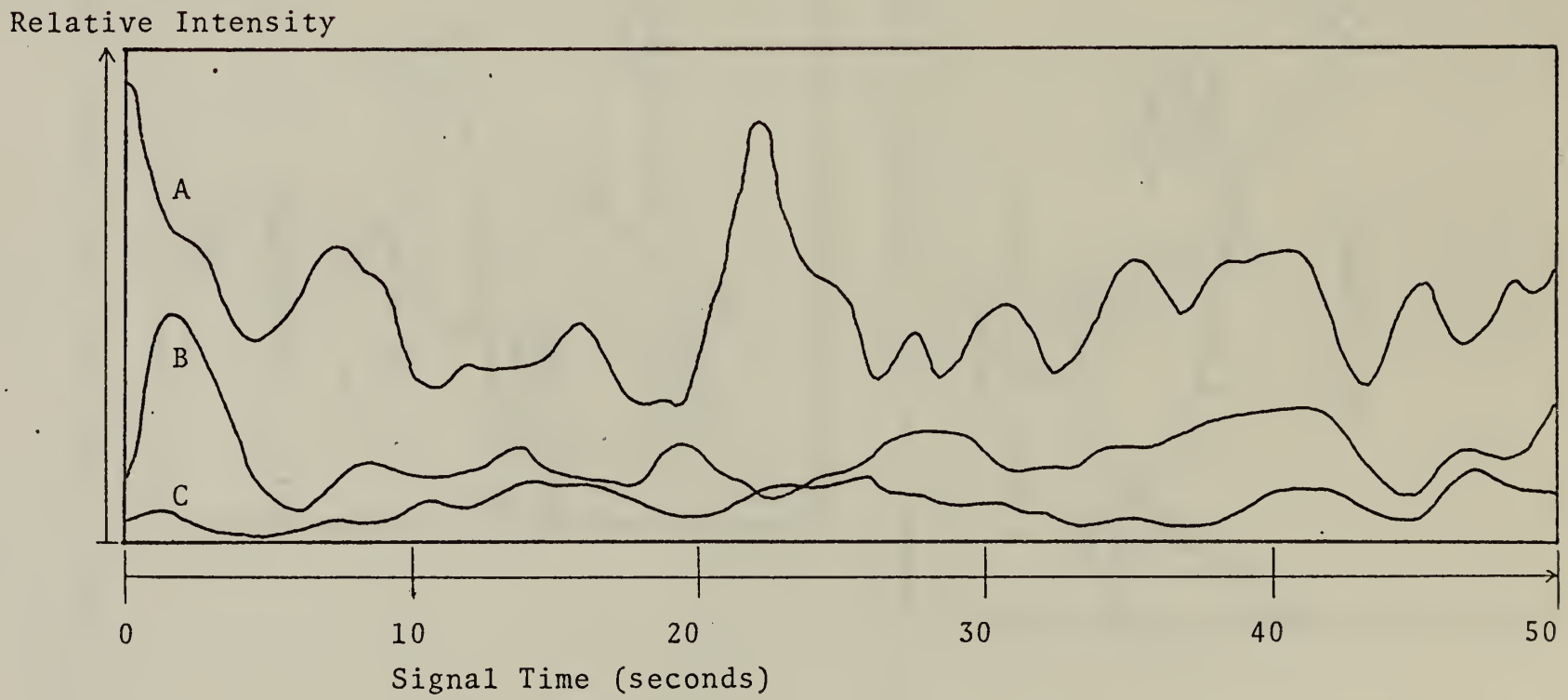

The graph shows the time variation of the relative intensity of three scintillation signal components (A, B and C). The average signal component intensity over a period of 50 seconds was measured by integrating the corresponding component curve with a planimeter. The frequencies were: A = 5 Hz; B = 30 Hz; C = 50 Hz.

Figure 8.

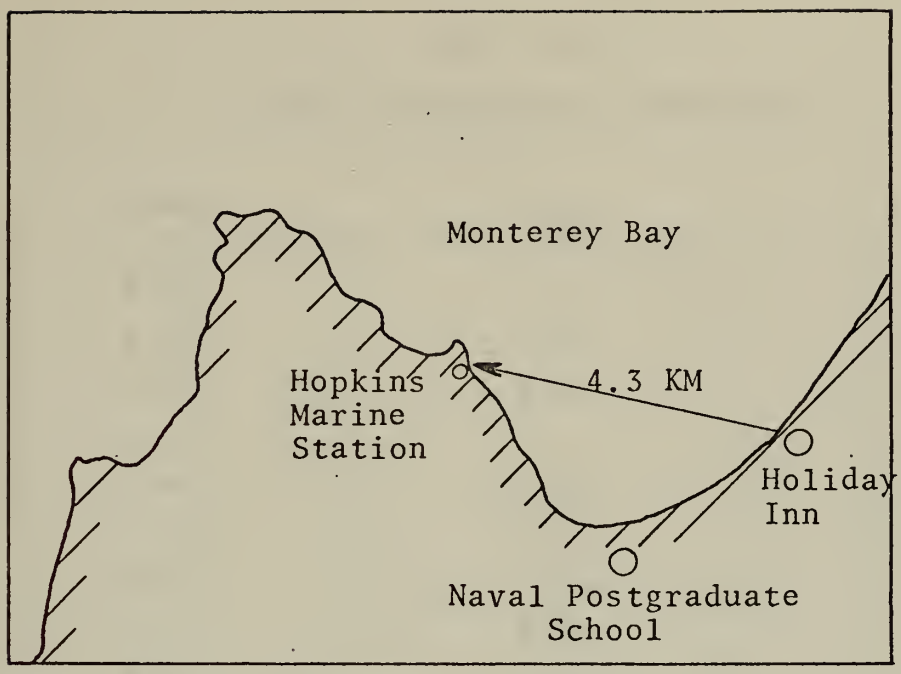

Figure 9. Laser Transmission Path over Monterey Bay.

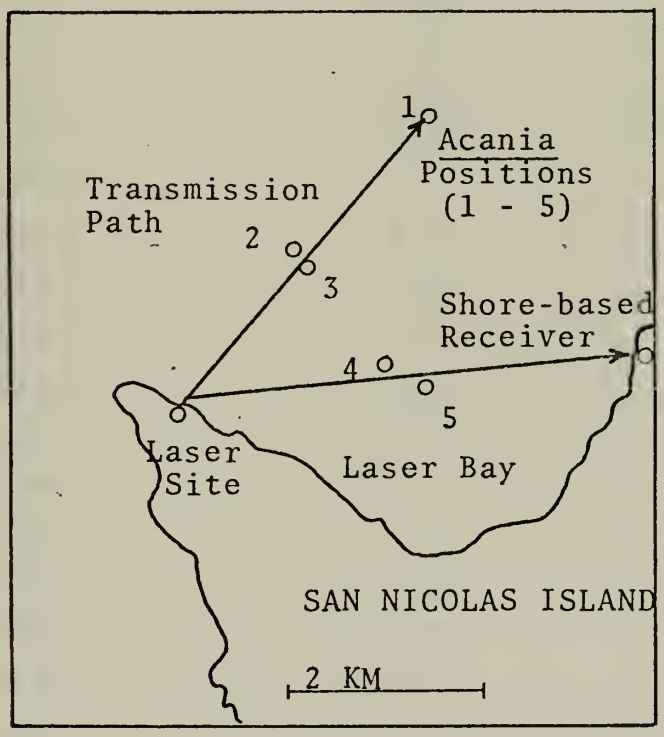

Figure 10. San Nicolas Island Experiment Transmission Paths.

APPENDIX C

DATA TABLE I

FIRST MONTEREY BAY EXPERIMENT

Time	C_{NO}	C_{NT}
1220	---	3.21
1225	2.87	2.80
1230	2.50	3.02
1235	---	3.56
1240	2.18	2.51
1245	2.55	2.80
1250	2.55	3.22
1255	2.66	3.60
1300	2.71	3.73
1305	2.98	3.11
1310	3.30	4.02
1315	3.57	2.80
1320	4.36	5.01
1325	4.15	12.00
1330	----	4.02
1335	3.25	4.50
1340	3.41	3.45
1345	---	3.53
1350	3.25	15.00
1355	---	5.01
1400	---	3.02
1405	3.00	2.03
1410	2.87	2.52
1415	2.93	3.73
1420	2.77	3.54
1425	---	3.01
1430	2.23	3.70
1435	2.34	3.00
1440	2.18	3.55

DATA TABLE I

FIRST MONTEREY BAY EXPERIMENT

Time	C_{NT}	C_{NT}
1445	2.18	3.11
1450	2.87	3.52
1455	2.55	2.91
1500	2.55	2.43
1505	2.55	2.72
1510	2.39	2.84
1515	2.18	2.45
1520	2.39	2.61
1525	2.55	4.10
1530	2.55	3.04
1535	2.55	1.40
1540	2.61	2.61
1545	2.61	3.51
1550	---	5.52
1555	---	4.51
1600	2.66	1.54
1605	2.71	3.40
1610	2.50	2.70
1615	2.39	2.51
1620	2.23	2.52
1625	2.29	4.23
1630	2.13	4.05
1635	2.18	---
1640	2.07	---
1645	2.39	---
1650	2.07	---
1655	2.02	---
1700	2.07	---

DATA TABLE II

SAN NICOLAS ISLAND EXPERIMENT

OPTICAL MEASUREMENTS		METEOROLOGICAL MEASUREMENTS	
TIME (PST)	$C_{NO}(x\ 10^{-8}m^{-1/3})$	TIME (PST)	$C_{NT}(x\ 10^{-8}m^{-1/3})$
Data by USNPS Group		Data by USNPS Group	
0440	5.2	0545	3.7
0445	4.4	0600	4.5
0504	6.0	0630	4.8
0555	2.2	0710	5.0
0605	3.7	0750	5.6
0610	2.4		
Data by NAVMISCEN Group			
0200	5.5		
0300	5.5		
0500	6.4		
0645	3.3		

DATA TABLE III

SECOND MONTEREY BAY EXPERIMENT

Time (2 May)	C_{NO}	C_{NT}
1400	---	15.0
1405	---	14.6
1410	6.01	14.6
1415	---	15.0
1420	5.60	14.6
1425	---	2.67
1430	5.52	3.46
1435	5.60	3.46
1440	5.79	3.58
1445	5.60	2.13
1450	---	---
1455	5.01	---
1500	5.34	---
1505	5.25	---
1510	6.21	---
1515	---	---
1520	---	---
1525	---	5.94
1530	---	4.81
1535	---	6.13
1540	---	5.33
1545	---	5.12
1550	5.01	2.67
1555	5.69	6.94
1600	5.90	5.26

DATA TABLE III

SECOND MONTEREY BAY EXPERIMENT

Time (2 May)	C_{NO}	C_{NT}
1605	5.31	5.33
1610	7.01	5.12
1615	---	4.61
1620	6.10	4.91
1625	6.72	4.29
1630	5.71	4.61
1635	---	4.61
1640	6.25	5.12
1645	---	4.30
1650	6.39	4.91
1655	---	4.81
1700	---	4.71
1705	---	5.12
1710	---	4.40
1715	---	5.02
1720	---	4.91
1725	5.70	4.81
1730	---	4.61
1735	---	4.74
1740	---	4.40
1745	4.91	4.71
1750	4.07	4.81
1755	4.35	4.30
1800	4.92	4.39

DATA TABLE III

SECOND MONTEREY BAY EXPERIMENT

Time (3 May)	C_{NO}	C_{NT}
1805	5.35	4.59
1810	---	4.59
1815	4.47	4.69
1820	4.77	4.59
1825	4.07	4.69
1830	4.49	4.69
1835	3.79	4.39
1840	3.51	4.59
1845	3.23	4.49
1850	3.65	4.39
1855	3.79	4.59
1900	4.57	4.69
1905	4.07	4.48
1910	4.07	4.28
1915	4.07	4.51
1920	3.93	4.48
1925	4.77	4.18
1930	4.50	---
1935	---	---
1940	3.79	---
1945	3.65	---
1950	3.65	---
1955	---	---
2000	---	---

DATA TABLE III

SECOND MONTEREY BAY EXPERIMENT

Time (3 May)	C_{NO}	C_{NT}
0630	2.72	---
0635	---	---
0640	2.25	---
0645	---	---
0650	---	---
0655	2.53	---
0700	2.53	---
0705	2.34	---
0710	2.06	---
0715	2.06	---
0720	1.59	---
0725	1.97	---
0730	2.34	2.31
0735	2.34	3.08
0740	2.15	1.95
0745	2.15	1.64
0750	2.25	3.60
0755	2.62	3.60
0800	2.62	4.01
0805	2.28	3.70
0810	2.15	3.17
0815	2.62	3.70
0820	2.81	3.91
0825	2.72	4.63
0830	2.72	5.14
0835	3.47	6.16
0840	3.56	9.37
0845	3.56	5.45
0850	3.56	8.03

DATA TABLE III

SECOND MONTEREY BAY EXPERIMENT

Time (3 May)	C_{NO}	C_{NT}
0855	3.84	6.49
0900	4.31	5.81
0905	4.12	5.10
0910	4.50	6.12
0915	4.31	4.90
0920	4.22	7.97
0925	3.84	6.12
0930	3.84	6.12
0935	---	5.10
0940	---	4.39
0945	---	4.49
0950	2.35	5.10
0955	2.97	7.97
1000	2.15	5.61
1005	---	3.82
1010	3.09	4.25
1015	3.09	4.25
1020	3.28	8.85
1025	3.28	8.85
1030	3.47	4.70
1035	---	4.27
1040	---	3.50
1045	4.22	4.19
1050	4.22	3.84
1055	3.71	3.93
1100	3.56	3.42

DATA TABLE III

SECOND MONTEREY BAY EXPERIMENT

Time (3 May)	C_{NO}	C_{NT}
1105	3.47	3.50
1110	3.47	3.67
1115	3.47	3.75
1120	5.15	3.84
1125	5.90	3.07
1130	---	3.59
1135	4.12	3.95
1140	4.03	3.85
1145	4.12	3.85
1150	4.87	4.14
1155	4.78	4.14
1200	4.31	3.73
1205	4.22	4.11
1210	3.94	3.92
1215	4.40	4.20
1220	4.03	4.11
1225	4.69	4.39
1230	4.69	4.20
1235	5.45	3.83
1240	5.70	4.48
1245	5.55	4.67
1250	4.31	4.67
1255	4.50	4.47
1300	4.03	4.29

DATA TABLE III

SECOND MONTEREY BAY EXPERIMENT

Time (3 May)	C_{NO}	C_{NT}
1305	4.03	3.92
1310	4.03	3.73
1315	4.12	4.20
1320	4.31	4.29
1325	4.40	4.39
1330	4.59	4.50
1335	4.50	4.69
1340	4.78	4.41
1345	4.12	4.41
1350	3.65	4.69
1355	3.47	4.31
1400	3.47	4.50
1405	3.56	4.50
1410	3.56	4.50
1415	3.56	4.41
1420	3.56	4.78
1425	3.92	4.69
1430	3.75	4.50
1435	3.47	4.50
1440	3.56	4.60
1445	---	4.50
1450	---	4.22
1455	3.34	3.94
1500	3.75	4.22

DATA TABLE III

SECOND MONTEREY BAY EXPERIMENT

Time (3 May)	C_{NO}	C_{NT}
1505	4.12	4.31
1510	4.03	3.94
1515	4.03	4.12
1520	4.03	3.75
1525	5.25	3.94
1530	---	4.41
1535	---	4.22
1540	4.40	4.13
1545	---	4.22
1550	---	4.22
1555	5.15	3.94
1600	5.05	4.12
1605	4.69	3.94
1610	3.75	4.31
1615	4.40	3.94
1620	---	3.75
1625	3.75	3.94
1630	4.12	4.24
1635	---	4.52
1640	---	2.82
1645	---	2.73
1650	---	3.18
1655	---	2.63
1700	---	2.82

DATA TABLE III

SECOND MONTEREY BAY EXPERIMENT

Time (3 May)	C_{NO}	C_{NT}
1705	---	3.01
1710	---	2.35
1715	---	2.07
1720	---	2.26
1725	---	2.35
1730	---	2.48
1735	---	2.48
1740	---	2.48
1745	---	1.88
1750	---	1.88
1755	---	2.06
1800	---	2.15
1805	---	2.24
1810	---	2.05
1815	---	1.86
1820	---	1.96
1825	---	1.86
1830	---	1.96
1835	---	1.68
1840	1.97	1.12
1845	1.87	1.68
1850	1.78	1.31
1855	1.68	2.01
1900	1.87	2.05

DATA TABLE III

SECOND MONTEREY BAY EXPERIMENT

Time (3 May)	C_{NO}	C_{NT}
1905	1.97	2.34
1910	2.06	2.34
1915	2.06	1.96
1920	2.25	2.38
1925	2.53	2.01
1930	2.72	1.87
1935	2.44	1.68
1940	2.53	1.22
1945	2.06	1.40
1950	2.25	1.78
1955	2.34	1.80
2000	2.34	1.68
2005	1.97	1.73
2010	1.78	1.31
2015	1.78	1.78
2020	1.68	1.63
2025	1.87	1.78
2030	2.06	1.63
2035	1.97	1.78
2040	1.87	1.87
2045	2.06	2.10
2050	1.96	2.29
2055	2.06	---
2100	1.69	---

BIBLIOGRAPHY

1. Tatarski, V. I., trans. by Silverman, R. A., Wave Propagation in a Turbulent Medium, McGraw-Hill Book Co., Inc., New York, 1961.

2. Dowling, J. A. and Livingston, P. M., "The Behavior of Focused Beams in Atmospheric Turbulence: Measurements and Comments on the Theory," paper presented at OSA meeting, from NRL Washington, Spring 1972.

3. Ochs, G. R., "Measurements of 0.63 μm Laser Beam Scintillation in Strong Atmospheric Turbulence," Environmental Science Services Administration ERL-154-WPL-10, December 1969.

4. Fitzmaurice, M. W., "Experimental Investigation of Optical Propagation in Atmospheric Turbulence," NASA TR-R-370, August 1971.

5. Middleton, W. K., "The Effect of the Angular Aperture of a Telephotometer on the Telephotometry of Collimated and Non-Collimated Beams," Journal of the Optical Society of America, Vol. 39, No. 576, 1949.

6. Middleton, W. K., Vision through the Atmosphere, University of Toronto Press, Toronto, Canada, 1952.

7. Chandrasekhar, S., "A Statistical Basis for the Theory of Stellar Scintillation," Monthly Notices of the Royal Astronomical Society, Vol. 112, 1952.

8. Mintzer, D., "Wave Propagation in a Randomly Inhomogeneous Medium," Journal of the American Acoustical Society, Vol. 25, Part I, pp. 922-927; Part II, pp. 1107-1111, 1953.

9. Muchmore, R. B., Wheelon, A. D., "Line-of-Sight Propagation Phenomena," Proceedings of the I.R.E., Vol. 43, October, 1955.

10. Wheelon, A. D., "Near Field Corrections to Line of Sight Propagation," Proceedings of the IRE, Vol. 43, pp. 1459-1466, October 1955.

11. Wheelon, A.D., "Radio Wave Scattering by Tropospheric Irregularities," Journal of Atmospheric and Terrestrial Physics, Vol. 15, pp. 185-205, 1959.

12. Chernov, L. A., Wave Propagation in a Random Medium, New York, McGraw-Hill Book Co., Inc., 1960.

13. Ochs, G. R.; Bergman, R. R. and Snyder, J. R., "Laser Beam Scintillation over Horizontal Paths from 5.5 to 145 Kilometers," ESSA Research Laboratories, February 1969.

14. Rytov, S. M., "Diffraction of Light by Ultrasonic Waves," Izv. Akad. Nauk SSSR Ser. Fiz. #2, 1937.

15. Obukov, A. M., "On the influence of atmospheric inhomogeneities on the propagation of light and sound," Izv. Akad. Nauk SSSR Ser Geofiz #2, 1953

16. Strohbehn, J. W., "Line-of-Sight Wave Propagation through the Turbulent Atmosphere," Proceedings of the IEEE, August 1968.

17. Lumley, J. L., Panofsky, H. A., The Structure of Atmospheric Turbulence, Interscience Monographs, Wiley and Sons, New York, 1964.

18. Davidson, K. L., "Considerations in Providing Atmospheric Conditions over the Sea with Respect to Optical Wave Propagation," NPS in-house report to EO/LT Committee, October 1972.

19. Wyngaard, J. C.; Izumi, Y.; Collins, S. A., "Behavior of the Refractive-Index-Structure Parameter near the Ground," Journal of the Optical Society of America, Vol. 61, No. 12, December 1971.

20. Panofsky, H. A., "The Structure Constant for the Index of Refraction in Relation to the Gradient of Index of Refraction in the Surface Layer," Journal of Geophysical Research, Vol. 73, No. 18, September 15, 1968.

21. Davidson, K. L., "Describing Meteorological Conditions for Optical Propagation," NPS Report to EO/LT Committee, unpublished, May 1973.

22. Schmeltzer, R. A., "Means, Variances and Covariances for Laser Beam Propagation through a Random Medium," North American Aviation E.O. Lab, December 1965.

23. Fried, D. L., "Propagation of a Special Wave in a Turbulent Medium," Journal of the Optical Society of America, Vol. 57, No. 2, February 1967.

24. Fried, D. L.; Seidman, J. B., "Laser Beam Scintillation in the Atmosphere," Journal of the Optical Society of America, Vol. 57, No. 2, February 1967.

25. Friehe, C. A., Gibson, C. H., and Dreyer, G., Abstract, Journal of the Optical Society of America, 62, p. 1340, 1972.

INITIAL DISTRIBUTION LIST

		No. Copies
1.	Defense Documentation Center Cameron Station Alexandria, Virginia 22314	2
2.	Library, Code 0212 Naval Postgraduate School Monterey, California 93940	2
3.	Professor O. Heinz, Code 61 Hz Department of Physics and Chemistry Naval Postgraduate School Monterey, California 93940	1
4.	Asst Professor A. W. Cooper, Code 61 Cr Department of Physics and Chemistry Naval Postgraduate School Monterey, California 93940	8
5.	ENS Brian C. Haagensen, USN 118 Warwick Drive, Apt. #61 Benecia, California 94510	1

UNCLASSIFIED

Security Classification

DOCUMENT CONTROL DATA - R & D

(Security classification of title, body of abstract and indexing annotation must be entered when the overall report is classified)

ORIGINATING ACTIVITY (Corporate author)	2a. REPORT SECURITY CLASSIFICATION
Naval Postgraduate School Monterey, California 93940	Unclassified
	2b. GROUP

REPORT TITLE

Laser Beam Scintillation in the Marine Boundary Layer

DESCRIPTIVE NOTES (Type of report and inclusive dates)

Master's Thesis; June 1973

AUTHOR(S) (First name, middle initial, last name)

Brian Christian Haagensen

REPORT DATE	7a. TOTAL NO. OF PAGES	7b. NO. OF REFS
June 1973	109	25

8. CONTRACT OR GRANT NO.	9a. ORIGINATOR'S REPORT NUMBER(S)
b. PROJECT NO.	
c.	9b. OTHER REPORT NO(S) (Any other numbers that may be assigned this report)
d.	

10. DISTRIBUTION STATEMENT

Approved for public release; distribution unlimited.

11. SUPPLEMENTARY NOTES	12. SPONSORING MILITARY ACTIVITY
	Naval Postgraduate School Monterey, California 93940

13. ABSTRACT

Intensity scintillation in a laser beam at 0.63 micrometers in the marine boundary layer has been studied over a 4.3 kilometer horizontal path across Monterey Bay and also from shore to ship at San Nicolas Island. Optical and micrometeorological measurements of the refractive index structure constant, C_N, agree to approximately one standard deviation giving values in the range of 2.0×10^{-8} to 5.0×10^{-8} (meters)$^{-1/3}$. Optical and meteorological data correlation improved as mean wind speed increased. Evidence was found to support the reported existence of a saturation region for the laser beam logarithmic amplitude variance.

DD FORM 1 NOV 68 1473 (PAGE 1)

S/N 0101-807-6811

UNCLASSIFIED

Security Classification

A-31408

KEY WORDS	LINK A		LINK B		LINK C	
	ROLE	WT	ROLE	WT	ROLE	WT
Atmosphere						
Optics						
Laser						
Scintillation						
Propagation						